5

Turbulence and Complexity of Magnetospheric Plasmas

Marius Echim[1], Tom Chang[2], Peter Kovacs[3], Anna Wawrzaszek[4], Emiliya Yordanova[5], Yasuhito Narita[6], Zoltan Vörös[6], Roberto Bruno[7], Wieslaw Macek[4], Kalevi Mursula[8], and Giuseppe Consolini[7]

ABSTRACT

Turbulent fluctuations are omnipresent in the terrestrial magnetosphere as well as in other planetary plasma systems. While the topic is broad and was largely treated in the past (see, for instance, the works of Borovsky and Funsten, 2003; Zimbardo et al., 2010; Ovchinnikov and Antonova, 2017), this chapter provides a review that covers under the same title some key facts on the current understanding of turbulence observed in the main regions of the magnetosphere, such as the magnetosheath, the plasma sheet, and the cusps. We briefly discuss basic theoretical building blocks (mainly phenomenological) to set the scene for a discussion on the experimental results obtained during the last two decades of magnetospheric research. Indeed, an unprecedented fleet of spacecraft, like Cluster, THEMIS and MMS, provides in situ observations of magnetospheric turbulence for various geomagnetic conditions. We also discuss similarities and differences with respect to solar wind turbulence. In addition, we review ideas stemming from modern interpretations of turbulence and plasma and field fluctuations, such as dynamical complexity, and emphasize the key questions still awaiting clarification.

5.1. INTRODUCTION

Random, chaotic behavior of flow pattern can commonly be observed in many fluid systems in our daily life and geophysical flows (rivers, oceans, and atmosphere). Even plasmas in near-Earth space exhibit random fluctuations in the flow velocity, density, and magnetic field. Eddies, propagating waves, and coherent structures interact with one another, and nonlinear structures evolve both in space and time in the magnetospheric plasmas.

In the classical view (Kolmogorov-like) turbulence implies that many scales of fluctuations are simultaneously present and that they nonlinearly interact generating an energy transfer from the larger scale to the smaller ones where dissipation occurs. The classical theory considers mainly the fully developed (strong) turbulence, which is incompressible, isotropic, homogeneous, and develops freely, without effects imposed by dissipation, external forces, or boundaries. The phenomenological description stems from the so-called "Richardson cascade" (Richardson, 1922). The energy is injected into the largest scales of the medium, then it is transferred through nonlinear interactions to smaller and smaller scales (inertial range) until reaching the kinetic range of scales, where it dissipates, as heat, for example. In the inertial range the energy transfer rate is scale-invariant,

[1]*Royal Belgian Institute for Space Aeronomy, Brussels Belgium; and Institute of Space Science, Magurele, Romania*
[2]*Massachusetts Institute of Technology, Cambridge, USA*
[3]*Mining and Geological Survey of Hungary, Budapest, Hungary*
[4]*Space Research Centre, Polish Academy of Sciences, Warsaw, Poland*
[5]*Swedish Institute of Space Physics, Uppsala, Sweden*
[6]*Space Research Institute, Austrian Academy of Sciences, Graz, Austria*
[7]*The National Institute for Astrophysics (INAF), Rome, Italy*
[8]*Department of Physics, University of Oulu, Oulu, Finland*

Space Physics and Aeronomy Collection Volume 2: Magnetospheres in the Solar System, Geophysical Monograph 259, First Edition.
Edited by Romain Maggiolo, Nicolas André, Hiroshi Hasegawa, and Daniel T. Welling.

DOI: 10.1002/9781119815624.ch5

i.e. it does not depend on scale, and it is determined only by the mean energy dissipation rate per unit mass. In the dissipation range, turbulence starts to depend on the viscosity as well. These are the main conjectures of the so called K41 theory (Kolmogorov, 1941) developed to describe neutral fluid turbulence. A consequence of the probabilistic description of the fluctuations for a fluid described by the Navier–Stokes equation leads, under strong hypothesis (see, e.g. Frisch, 1995), to the derivation of a scaling law for the energy spectrum: in the inertial range the power scales as $f^{-\alpha}$ where $\alpha = 5/3$. The main assumptions made in K41 are the self–similarity, the localness of interactions in the inertial range, and a constant uniform energy transfer rate. Self-similarity refers to the space filling – the largest (mother) eddies breakdown into smaller (daughter) eddies, which occupy the same space volume as mother eddies, and this picture is valid for all scale sizes in the inertial range. The localness of the interactions means that the energy transfer is preferable for scales with comparable size. The power-law spectrum and the index value have successfully been tested against various turbulence experiments (e.g., Fig. 9 in Saddoughi and Veeravalli, 1994).

Turbulence evolves when the Reynolds number becomes sufficiently large, say 1000 or even higher (Frisch, 1995), when the flow nonlinearity (advection) exceeds the effects of viscosity. Random flow motions in turbulence serve as effective diffusion (or turbulent diffusion) of the large-scale, mean flow. In other words, turbulence mixes the flow efficiently, even much more than the molecular viscosity does. The Navier–Stokes equation is nonlinear in the flow velocity and cannot be directly time-integrated. However, the statistical quantities such as energy spectra or velocity correlations can be estimated. For example, Kolmogorov (1941) obtained a solution for the third-order moment of the flow velocity; Kraichnan (1965a, 1965b) derived the inertial-range spectrum using a closure approximation without introducing a free adjustable parameter (LHDIA, Lagrangian History Direct Interaction Approximation), which was extended to an inhomogeneous turbulence treatment (TSDIA, Two-Scale Direct Interaction Approximation) by Yoshizawa (1984, 1998).

In the ideal magnetofluid, incompressibility is maintained by the magnetic field strength (magnetic pressure). The presence of a strong background magnetic field in plasma produces fluctuations propagating as Alfvén waves parallel and antiparallel along it. As a result, only Alfvén waves traveling in opposite directions interact. Since the flow velocity is much lower than the Alfvén speed, the waves' interaction time is shorter than the eddy distortion time. This decorrelation is the basis of the Alfvén effect (Biskamp, 1993), and it results in slower full energy transfer in magnetohydrodynamic (MHD) turbulence (α=3/2). The corresponding energy spectrum of MHD turbulence, Iroshnikov–Kraichnan (IK67) (Iroshnikov, 1963; Kraichnan, 1965a, 1965b), depends not only on the energy transfer rate but on the Alfvén velocity as well. The energy cascade is anisotropic, being faster along the perpendicular than along the parallel wave numbers. When turbulence becomes strong, the so-called critical balance is achieved between parallel (linear) and perpendicular (nonlinear) energy propagation, which is at the base of Goldreich and Sridhar (1995) phenomenology (see also Narita, 2016a).

Turbulence in near-Earth space is unique in that it occurs in a collisionless, magnetized plasma. This fact imposes many challenges toward understanding of magnetospheric plasma turbulence. First, turbulent flows are closely coupled to the electric and magnetic fields. Not only eddies (which inherit fluid turbulence) but also propagating electromagnetic waves are the ingredients of plasma turbulence and there is a higher degree of freedom in a turbulent cascade mechanism. Simultaneous coexistence of propagating modes and intermittent nonlinear spatiotemporal structures is the norm of the states of the plasma media in the space environment. Recent results demonstrate that the physics of the bimodal state of admixtures of such types of turbulent fluctuations may be understood from the point of view of the development and interactions of coherent structures arising from sporadic and localized plasma resonance sites (Chang et al., 2004).

Second, energy dissipation needs to be achieved without binary collisions or viscosity, through heating of particles. One possible scenario involves resonant damping of electromagnetic fluctuations at kinetic scales leading to an increase of entropy, thus to dissipation in the thermodynamic sense. Ion and electron Landau damping of kinetic Alfvén waves is a possibility explored theoretically and with data analysis (Leamon et al., 1999; Sahraoui et al., 2009; Borovsky and Gary, 2011; Chen et al., 2019). As an alternative, nonlinear perpendicular phase mixing sustains an entropy cascade and leads also to energy dissipation (Schekochihin et al., 2008). Another relevant process is the nonresonant, stochastic damping of waves whose dissipative effect is the broadening of particle velocity distribution (Johnson and Cheng, 2001; Voitenko and Gossens, 2004). Plasma structures like current sheets (Sundkvist et al., 2007), Alfvénic vortices (Alexandrova et al., 2006), and electrostatic forms (Stawarz et al., 2015) are also believed to play a role in dissipation of space plasma turbulent energy. Anomalous transport and diffusion of energy at coarse-grained scales (Wu and Chang, 2001) may also serve as effective dissipation mechanisms.

Third, the presence of the mean magnetic field brings about anisotropy in turbulence processes, e.g., anisotropy in wave propagation direction and energy cascade

mechanism (Narita, 2015). On larger spatial scales, when the gyro-motion of the ions is safely neglected, the plasma motion can be approximated to that of a magnetofluid (magnetohydrodynamics, MHD). On smaller spatial scales, gyro-motion and wave particle energy exchange become important and the plasma needs to be treated kinetically and separately for the plasma species. In this chapter we treat recent results obtained from the analysis of spacecraft data in turbulence regions of the terrestrial magnetosphere. We aim to provide a map of turbulence properties and characteristics in three main magnetospheric regions: the magnetosheath, the magnetotail, and plasma sheet and the cusps and auroral regions. Let us first briefly summarize some of the main lessons learned from in situ investigation of solar wind turbulence.

5.2. LESSONS LEARNED FROM STUDIES OF SOLAR WIND TURBULENCE

Extensive studies based on data from various space missions as well as theoretical insights built a framework for understanding solar wind plasma turbulence (see, e.g., Bruno & Carbone, 2013; Alexandrova, 2008 and references therein) that can be relevant for magnetospheric turbulence. Nevertheless, the conditions in the solar wind are fundamentally different from the magnetospheric ones. The solar wind turbulence may be considered fully developed, particularly at relatively large distances from the Sun, the interactions with boundaries are of minor importance, and the Reynolds number is quite high. The solar wind is often called the largest natural turbulence tunnel (Bruno and Carbone, 2013).

The Power Spectral Density of solar wind fluctuations exhibit power-law ranges, separated by spectral breaks, as illustrated in Figure 5.1. Numerous studies confirm an f^{-1} spectrum at large scales as well as a Kolmogorov scaling ($f^{-5/3}$ spectrum) in the inertial range (Leamon et al., 1998; Wicks et al, 2010). However, the size of the inertial range, in particular, the location of the high-frequency break, depends on the solar wind conditions and varies with the heliocentric distance, moving to lower frequencies as the wind expands, suggesting a cyclotron-resonant dissipation mechanism (Bruno and Trenchi, 2014).

Moreover, at frequencies above the high-frequency break the spectrum steepens from f^{-2} to f^{-4}, a spectral behavior associated by some authors to different physical processes: ion cyclotron resonances (Leamon et al. 1998); kinetic Alfvén waves (Sahraoui et al., 2009), dissipation at electron scales (Alexandrova et al., 2009; Chen et al., 2012); Hall effect or ion cyclotron damping of obliquely propagating fluctuations (Alexandrova et al., 2012; Bourouaine et al., 2012). On the other hand, Bruno et al. (2014) showed that the spectral slope at frequencies higher than the spectral break is strongly related to the wind speed and to the power of the fluctuations within the inertial range.

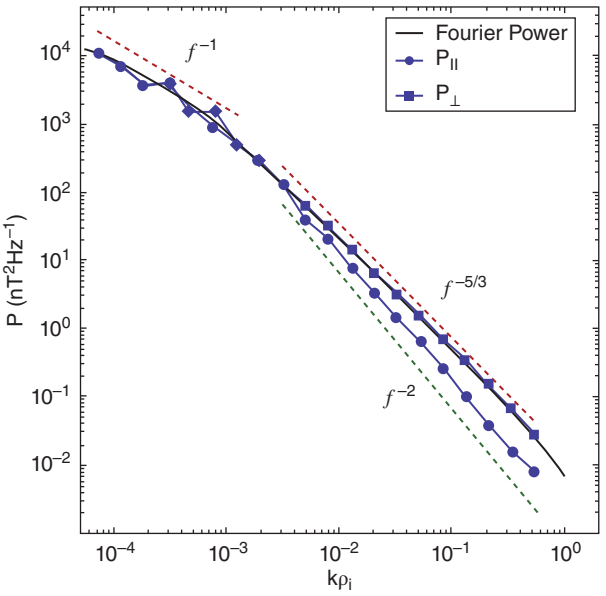

Figure 5.1 Trace of the wavelet and Fourier power spectra of magnetic field observations from Ulysses for the period between days 100 and 200 of 1995. Figure published by Wicks et al. (2010).

Another important feature of the small-scale solar wind fluctuations is the presence of intermittency, identified by the departure of probability density functions (PDFs) from Gaussian statistics (Marsch and Tu, 1994; Sorriso-Valvo et al., 1999), anomalous scaling of structure functions (Burlaga 1991) or from multifractal analyses (Macek and Wawrzaszek, 2011; Wawrzaszek et al., 2015, 2019). The intermittent character of magnetic field fluctuations in the kinetic range has also been investigated (Kiyani et al., 2009; Perri et al., 2012; Wan et al., 2012; Carbone et al., 2018; Alberti et al., 2019). Results seems to indicate that although there is a clear departure from Gaussianity of the PDFs of the fluctuations/increments in the kinetic domain, there is, however, a quasi-self-similarity of these fluctuations, i.e., the multifractal character and the anomalous scaling features are lost.

The turbulence of undisturbed solar wind is highly anisotropic in the inertial range (Horbury et al. 2008, Wicks et al., 2010) as well as at kinetic scales (Lacombe et al., 2017). The anisotropy is revealed by the spectral behavior of magnetic field fluctuations and seems to depend strongly on the large-scale magnetic field (Sorriso-Valvo et al., 2010) or plasma beta (Bruno and Carbone, 2013).

One key hypothesis to understand turbulence, the Taylor frozen-in-flow hypothesis, is usually satisfied in the solar wind at MHD scales. Some studies suggest that this hypothesis may fail when the solar wind flow velocity falls below the Alfvén wave velocity, and when dispersive effects at small scales cause the wave frequency to increase more rapidly than linearly with the wavevector (Howes et al, 2014, Perri et al., 2017).

Unlike weak turbulence, strong turbulence as described in the introductory section of this chapter cannot be understood purely in terms of waves and wave interactions alone. Although any fluctuation may be mathematically expanded in terms of sines and cosines, when inserting such expansions into the basic fluid and/or kinetic plasma equations the nonlinear terms in the equations will generate infinite number of interaction terms that must be considered in full in a strong turbulence analysis. To circumvent such difficulty, there exist special methods, such as fractals, wavelet transforms, structure function, singularity and rank-ordered spectrum procedures, and other related theoretical techniques, to address and analyze strong turbulence involving the bimodal dynamic interactions of coherent structures and wave modes. Some of these ideas are discussed in more detail in the illustrative examples of this chapter.

5.3. TURBULENCE AND COMPLEXITY IN KEY MAGNETOSPHERIC REGIONS

Fleets of spacecraft orbiting along highly elongated trajectories allow in situ investigation of turbulence in virtually all magnetospheric domains. In the following sections some of the main results obtained during the last decades are reviewed and the main similarities and differences between turbulence properties in key magnetospheric regions are emphasized.

5.3.1. Bow Shock, Shock-Upstream, and Magnetosheath Turbulence

Terrestrial bow shock (BS) results from the interaction of the supersonic and superalfvénic solar wind flow with the outer layers of the Earth's magnetic field and plasma. The large-scale properties of the bow shock are controlled by θ_{Bn} (the angle between the upstream interplanetary magnetic field (IMF) and the normal to the bow shock surface) the magnetospheric system size and the Mach number. When θ_{Bn} is smaller than 45°, the configuration is called quasi-parallel (Qpar), as opposed to the quasi-perpendicular (Qperp) case where the angle is larger than 45°.

The upstream region of the BS where the solar wind is magnetically connected to the BS surface is called foreshock. The foreshock is the subject of a number of instabilities emerging between incoming solar wind particles and ions and electrons reflected from the bow shock surface along the IMF lines. Instabilities result in the excitation of ultralow frequency (ULF) waves and various nonlinear structures, such as shocklets, Short Large Amplitude Magnetic Structures (SLAMS, Schwartz et al., 1992), hot flow anomalies (HFAs), spontaneous HFAs (Zhang et al., 2013 and references therein). Despite the well-known subdivision to ion and electron foreshock, recently it has been reported that the ion foreshock is bounded by compressional boundaries of enhanced magnetic field and density (Rojas-Castillo et al., 2013). There are also traveling foreshocks caused by consecutive rotations of the IMF that change locally the bow shock geometry and bound a region exhibiting fluctuations similar to the foreshock ones (Kajdic et al., 2017).

The quasi-parallel shock is the region where the strongest turbulence is observed and the fluctuations in all parameters are intensified. Due to the downstream-convected foreshock fluctuations, the quasi-parallel shock surface is strongly rippled and the local curvature variations can generate fast jets penetrating to the magnetosheath (Hietala and Plaschke, 2013). The turbulent fluctuations at quasi-perpendicular shock have lower amplitudes. However, they are the efficient source of particle energization at kinetic scales (Johlander et al., 2016). Very recent detection of rippling in the quasi-perpendicular bow shock has been accounted responsible for the observed reflection of ions (Johlander et al, 2018).

The magnetosheath (MSH) is bounded by the bow shock and the magnetopause (MP). Its spatial extent in the subsolar region is of the order of 3 R_E. (R_E being the Earth' radius). The main dynamical and turbulent features are determined by the geometry of the upstream part of the bow shock, i.e., its Qpar or Qperp character. The Qpar magnetosheath exhibits strong turbulence where the $\delta B/B$ ratio is close to unity. On the contrary, the power of the electromagnetic fluctuations behind the quasi-perpendicular part of BS is about one order weaker (Figure 5.2). Though the main part of the MSH plasma is composed of solar wind (SW) particles, the physical conditions change considerably behind the BS. As compared to the SW, the MSH plasma density increases (though it still remains collisionless), the plasma velocity is slowed down, the plasma beta exhibits a considerable spatiotemporal variation ranging from less than unity to order of ten, the ion temperature becomes much larger than that of electrons and there appears a big anisotropy between parallel and perpendicular temperatures as $T_\perp \gg T_\parallel$.

The release of strong temperature anisotropy in the collisionless MSH environment can take place only via wave particle interactions (Schwartz et al., 1996). The MSH dynamics characterized by large variations of the ion beta

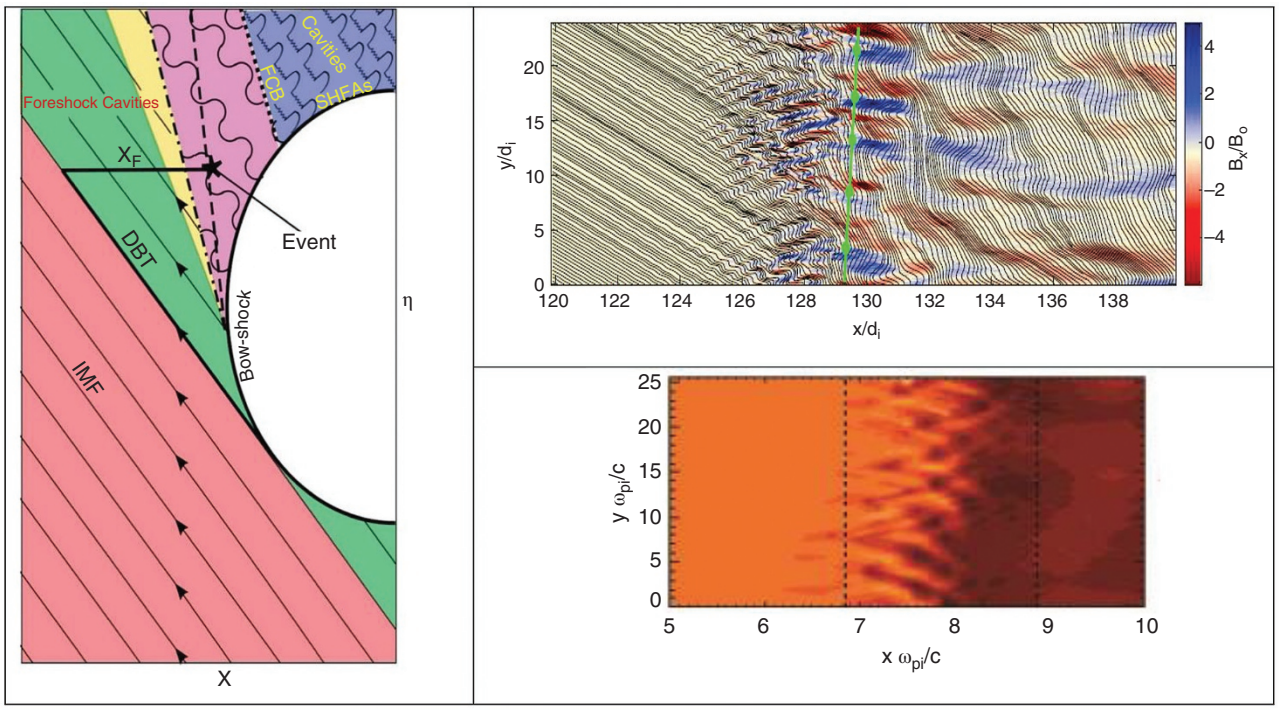

Figure 5.2 Left: schematic illustration of the shock geometry and associated upstream phenomena. The red and green regions illustrate a quasi-perpendicular geometry and the other regions correspond to quasi-parallel shock (figure published by Kajdic et al., 2017). Upper right: rippled magnetic structures at the quasi-parallel shock from hybrid simulations (Gingell et al., 2017) Lower right: rippled magnetic structures at the quasi-perpendicular shock from hybrid simulations (Burgess et al., 2016).

can be modelled by kinetic theory. It is argued that the temperature anisotropy, $T_\perp \gg T_{||}$, introduced by the shock ramp is the source of two basic linear wave modes, the Alfvén ion cyclotron (AIC) and mirror waves (Alexandrova et al., 2004; Sahraoui et al., 2003; Schwartz et al., 1996). AICs are dominant for low β_i and large temperature anisotropy environment while mirror modes require a high β_i and small temperature anisotropy satisfying the $\frac{T_\perp}{T_{||}} - 1 \geq 1/\beta_i$ condition. The highest growth rate of AIC instabilities is found for parallel propagation. When alpha particles are present the waves emerge in two different frequency bands related to the cyclotron frequencies of protons and He ions, respectively (Gary et al., 1994). The mirror waves are compressional nonpropagating waves with zero frequency in the plasma rest frame. In general, at low and intermediate frequencies (1 - 100 mHz) AIC waves are more dominant near the weak quasi-perpendicular BS and in the plasma depletion layer, while mirror modes dominate the region at middle magnetosheath (Schwartz et al., 1996, Sahraoui et al., 2003).

In a case study Sahraoui et al. (2003, 2006) applied the k-filtering technique (Pincon and Lefeuvre, 1991) on Cluster multispacecraft data in high-beta plasma near the magnetopause and showed that magnetic fluctuations related to different spacecraft frequencies correspond to mirror waves of different spatial scales, i.e. wave numbers. The largest mirror structure appears at f_{sc} = 0.11 Hz corresponding to $k\rho \sim 0.3$ (ρ being the proton Larmor radius), i.e. a spatial scale of about 2,000 km and the structure can be followed until f_{sc} = 1.5 Hz and $k\rho \sim 3.5$ (~150 km) (Sahraoui et al., 2006). Since the small-scale mirror waves should have been damped according to the kinetic linear theory it is argued that nonlinear effects are at work while cascading the energy from large to small spatial scales. This process is however not isotropic and proceeds to full development only along the plasma flow direction, k_v. The magnetic energy spectrum in terms of k_v can be obtained by consecutive space–time integration of the four dimensional $B^2(\omega, \boldsymbol{k})$ power function over frequency and over directions perpendicular to the flow. The reduced spectrum exhibits power-law behavior, $k_v^{-8/3}$, that is valid for the full wave number range ($0.3 < k_v\rho < 3.5$), i.e. no spectral break is observed.

Although the general plasma conditions change rapidly in the magnetosheath, the environment is highly inhomogeneous and the upstream and downstream boundaries are relatively close, some universal properties of MSH plasma and field fluctuations have been found. Czaykovska et al. (2001) showed that irrespective of the quasi-parallel or quasi-perpendicular geometry

of the bow shock, the magnetic variations in the MSH exhibit broken power-law spectra. Breuillard et al. (2016) argued that the spectral break at kinetic scales is closer to the smallest ion characteristic scale, the gyroradius ρ_i or the inertial length λ_i, for various plasma conditions ($0.5 \leq \beta \leq 10$). However, at low frequencies the scaling exponent is close to −1, a common feature with solar wind magnetic field spectra where the 1/f scaling is believed to be related to the superposition of uncorrelated magnetic structures emerging from the solar surface and having log-normal distribution of correlation lengths (Matthaeus and Goldstein, 1986). At high frequencies the power-law index in the magnetosheath is between −2 and −3. Breuillard et al. (2016) also showed that the occurrence of AIC or mirror/slow mode waves result in less steep spectra at small scales, otherwise the scaling exponent is close to −2.8 consistent with kinetic Alfvén wave (Howes et al., 2008; Schekochihin et al., 2009), whistler modes (Stawicki et al., 2001) or Hall-MHD turbulence (Alexandrova et al., 2007) scenarios.

In medium or low β plasma environments, the steep part of the spectra is often preceded by bumps in the vicinity of frequencies typical for kinetic instabilities (Alexandrova et al., 2006; Breuillard et al., 2016). Alexandrova (2008) argued that the bump feature is different from what is expected for the peak signature of linear wave modes and conjectured that in case of ion cyclotron instabilities the bumps are related to the emergence of Alfvén vortices (Petviashvili and Pokhotelov, 1992), that are shown to be the solutions of the incompressible ideal MHD equations. Alfvén vortices are incompressible coherent field-aligned current structures with small (near to the ion Larmour radius) dimension perpendicular to the ambient magnetic field and with transversal magnetic field and velocity fluctuations. Alexandrova et al. (2006) pointed out several possible mechanisms for the generation of the Alfvén vortices; however, the question remained open as to which mechanism is the most probable in the magnetosheath region. In the paper of Alexandrova et al. (2008) it is argued that a network of monopole or dipole filamentary vortices can satisfactorily explain the spectral features observed in the magnetosheath, namely the flat and steep part at large and small scales, respectively, as well as the spectral bump around the frequencies separating the two scaling regions. A striking recurrent feature of the magnetic field spectra in the subsolar magnetosheath region and near the BS is the apparent lack of a properly defined inertial range at MHD scales (below the proton gyrofrequency, f_{ci}). Indeed, Huang et al. (2017) showed that magnetic field spectra depart significantly from the $f^{-5/3}$ (Kolmogorov) or $f^{-3/2}$ (Iroshnikov–Kraichnan) scaling typically observed for inertial range turbulence (Figure 5.3). This finding is in contrast with the spectral properties of fully developed solar wind turbulence and could imply that downstream the BS new fluctuations are generated independently on the solar wind turbulent structures (Huang et al., 2017).

Hybrid simulations and recent MMS observations seemed to confirm this behavior (Gingell et al., 2017). However, it was also suggested that the random-like field observed just behind the BS can later develop into correlated fluctuations exhibiting Kolmogorov-like features if there is enough time for the nonlinear interactions and the cascade can involve larger and larger ranges of scales. This process seemed to be verified by the observations of $f^{-5/3}$ inertial range magnetic field spectra in the flank regions of the magnetosheath at large distances from the shock surface (Alexandrova, 2008; Huang et al., 2017; see also Dwivedi et al., 2019). Note also an alternative explanation for the emergence of developed turbulence in the flank regions of the magnetosheath that considered the cascade initiated by large-scale coherent structures developed on the flank of the magnetopause by Kelvin–Helmholtz instability (Hasegawa et al., 2004; Karimabadi et al., 2014).

The properties of the plasma fluctuations beyond the MHD scale, at electron ($kc/\omega_{pe} = \sim 0.3 - 30$, where ω_{pe} is the electron plasma frequency) and electrostatic (kc/ω_{pe}~30 − 200) scales, were investigated through the joint spectra derived from FGM magnetic field (Balogh et al., 2001) and STAFF spectral analyser (Cornilleau-Wehrlin et al., 2003) records of the Cluster spacecraft. Note that the given frequency range corresponds to scales of the order of 0, 1 − 10 km, much smaller than the spacecraft separation; therefore only single spacecraft analyses could be applied. Considering that the spectra of MSH electromagnetic (δB^2 and δE^2) fluctuations have a dominant $f^{-\alpha}$ power-law dependence, and that the observed spacecraft frame frequencies are the Doppler shifts of the plasma frame frequencies, $f = f_0 + \boldsymbol{k} \cdot \boldsymbol{V}$ ($\boldsymbol{V}$ and $\boldsymbol{k}$ being the bulk plasma flow velocity and wave vector, respectively), it is argued that in case of anisotropic k distribution the δB^2 and δE^2 spectral values are functions of Θ_{BV} the angle between the ambient magnetic field **B** and the flow velocity **V**. By modeling the observed $\delta B^2(\Theta_{BV})$ and $\delta E^2(\Theta_{BV})$ functions at different frequencies for the flank MS region, Mangeney et al. (2006) concluded that the plasma fluctuations exhibited two-dimensional (2-D) wave vector distribution with $k_\perp \gg k_\parallel$ and vanishing rest frame frequency, f_0, while the wave number dependence of the δB^2 magnetic fluctuations was $k^{-\nu}$ with $\nu = \sim 3 - 4$, at the electromagnetic range. Alexandrova et al. (2006) have shown that this scaling is valid both for compressional and transversal fluctuations, $\delta B_\parallel$ and $\delta B_\perp$, independent of the ion plasma β_i parameter. It is also shown that the 2-D turbulence range increased towards larger scales (smaller wave numbers) with β_i. This spectral behavior could be linked to mirror or slow mode waves; however it was stressed that results of several case studies are inconsistent with linear wave mode approximation (Mangeney et al.,

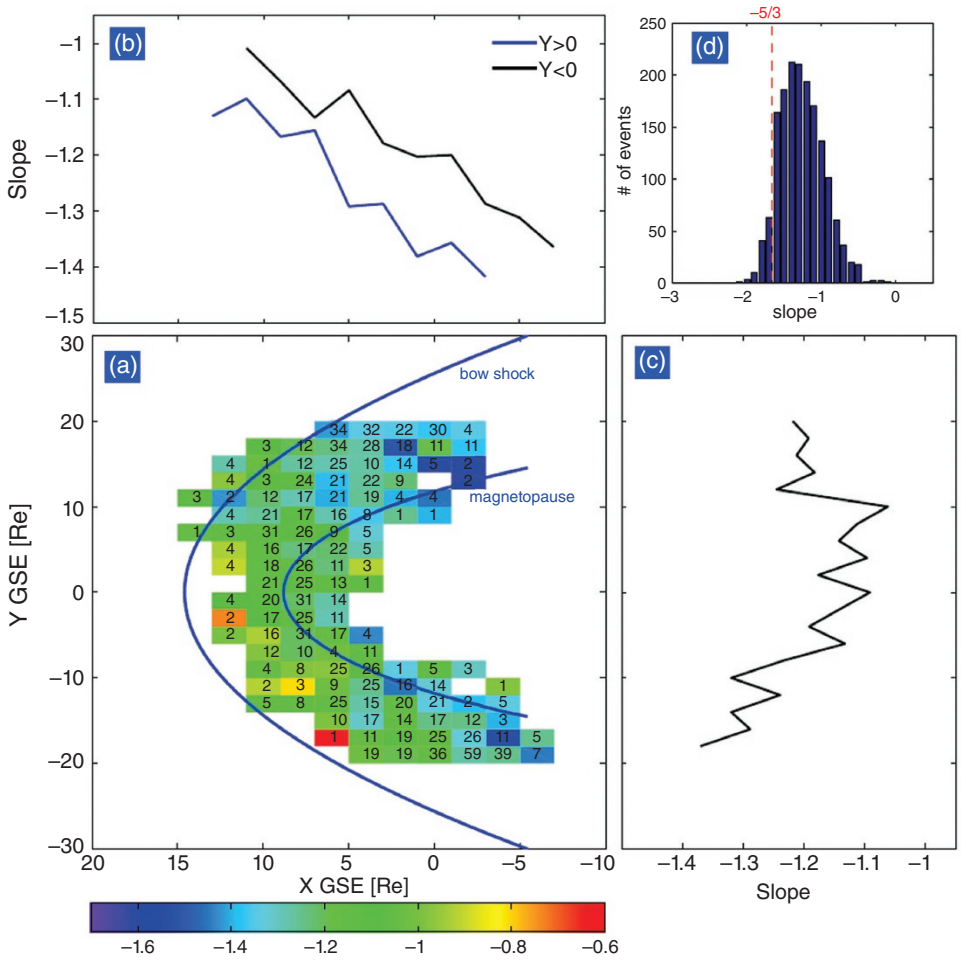

Figure 5.3 (a) The spatial distribution of spectral slopes detected at MHD scales from Cluster observations of magnetic field fluctuations in the Earth's magnetosheath (Huang et al., 2017); (b) the reduced distribution of spectral indices, integrated along positive/negative GSE Y (blue/black curves); (c) same as (b) but integrated along GSE X coordinate. The slope values are color code in panel (a) while the numbers represent the number of events exhibiting the given slope. It is shown that the MHD scale spectra steepen towards high $|Y_{GSE}|$ and small X_{GSE} coordinates, i.e. in the flank region. Kolmogorov spectra are observed in the flank, near to the magnetopause. The histogram of all spectral indices is shown in panel (d). Figure published by Huang et al. (2017).

2006) and point toward a nonlinear evolution of the electromagnetic fluctuations in the magnetosheath. Recent MMS magnetic observations that show a clear break of the magnetic spectrum exponent to about −11/2 at frequencies of 20–25 Hz agree with the predictions of kinetic theory (−16/3) (Macek et al., 2018a).

Another remarkable signature of universal MSH dynamics is intermittency, i.e. breaking of self-similarity of the turbulent cascade energy flow. Observations show that the energy is not distributed homogeneously and is dominated by nonlinear structures (shocklets, vortices, magnetic islands, cavitons, SLAMS, etc.) resulting in sudden intermittent changes in the electromagnetic fluctuations. The intermittent events lead to a departure from the Gaussian statistics at small scales. Therefore, their investigation needs higher-order moments of the fluctuating fields via, e.g., probability density function analysis (Macek et al., 2015, 2018b), gradient tensor geometrical invariants (Consolini et al., 2015; Quattrociocchi et al., 2019), structure function analysis or wavelet transform modulus maxima method (Yordanova et al., 2008). Concerning the spatiotemporal variation of intermittency behind the Qpar BS, Yordanova et al. (2008) verified that intermittency increases with the distance from the shock surface, and this finding is assigned to the effect of strengthening of the mean field and weakening of the fluctuations. The authors also showed stronger intermittency in the plane perpendicular to the mean field than in the parallel direction, suggesting an anisotropic development of the intermittent processes.

Intermittency is considered to be also effective for energy dissipation at kinetic scales, as well as for particle heating and acceleration. Kinetic simulations (Karimabadi et al., 2014), as well as experimental results for solar wind (Osman et al., 2011) and magnetosheath (Chasapis et al., 2015, 2017; Sundkvist et al., 2007), indicated that ion and electron heating can take place most effectively in current sheet structures. Magnetic discontinuities and current sheets can easily develop in turbulent media by nonlinear interaction of migrating flux tubes (Yordanova et al., 2008); therefore they seem to be abundant in Qpar magnetosheath (Vörös et al., 2017). Some of the current sheets are associated with magnetic reconnection. Recently, reconnection events have been identified in the magnetosheath also in kinetic scales by using Cluster (Retino et al., 2007; Phan et al., 2007) and MMS (Yordanova et al., 2016; Vörös at al., 2016) electromagnetic and plasma data. The case studies indicated that the magnetosheath turbulence is essential in triggering or generating reconnection at thin current sheets (Vörös et al., 2016).

5.3.2. Magnetotail and Plasma Sheet Turbulence

Driving, dynamics and dissipation of turbulence in the plasma sheet and magnetotail raise several open questions (Borovsky and Funsten, 2003): (1) how is energy transferred in plasma sheet turbulence? (2) what is the role of eddy-diffusion? (3) how do charged particles interact with turbulence? (4) what is the nature of the coupling between the plasma sheet turbulence and the ionosphere? and (5) which processes are involved in dissipation of turbulent energy? Borovsky and Funsten (2003) note that key hypothesis of classical MHD turbulence models (Kolmogorov, Iroshnikov–Kraichnan) might be violated in the plasma sheet and magnetotail due to: (i) the role of boundaries (e.g. the plasma sheet boundary layer), (ii) the spatial scales for turbulence driving and dissipation not being well separated, and (iii) the energy transfer rate not being scale invariant. Let us follow Borovsky and Funsten (2003) and investigate the current status of understanding for three key elements of plasma sheet and magnetotail turbulence.

Dynamics of Turbulence in the Plasma sheet and Magnetotail. Since the difference between the transversal size of the plasma sheet and the scales relevant for dissipation (ion Larmor radius and inertial length) is less than two decades the formation of a "proper" inertial range is questionable. Therefore, the paradigm of MHD turbulence in an homogeneous medium might not be appropriate; perhaps plasma sheet and magnetotail turbulence shows features similar to turbulence in a channel (Hussain and Reynolds, 1975) or the wake behind an obstacle (Taneda, 1956; Canuto and Taira, 2015) similar to neutral fluids dynamics or alternatively "turbulence-in-a-box" (Borovsky and Funsten, 2003). Another possible consequence is that turbulence in the magnetotail and plasma sheet might be dominated by flow eddies (2-D turbulence) rather than Alfvén waves (slab turbulence). Observations from THEMIS spacecraft and results of MHD simulations partially confirmed the dominance of eddies (Stepanova et al., 2011; El-Alaoui et al., 2013, 2016).

Driving of Turbulence in the Plasma Sheet and the Magnetotail. Fluctuations of magnetic field and plasma velocity are omnipresent in the plasma sheet and the magnetotail; their intensity depends on the geomagnetic activity while the level of magnetic fluctuations increases with increasing velocity fluctuations (Neagu et al., 2002, 2005). Whether these fluctuations can be directly related to turbulence is not yet clarified. Nevertheless, several mechanisms for driving turbulence in the plasma sheet and the tail are considered (see also Table 2 of Borovsky and Funsten, 2003): (1) Bursty Bulk Flows (BBFs); (2) Low-Latitude-Boundary-Layer (LLBL) shear flow; (3) shears in large-scale tail flow; (4) turbulent and sporadic reconnections; and (5) global reorganization of the plasma sheet state as in critical phase transitions (driven and/or self-organized criticality). These mechanisms are briefly reviewed here.

Bursts of perpendicular sunward plasma (bursty bulk) flows often observed in the plasma sheet carry significant amounts of mass and momentum (Baumjohann et al., 1989; Angelopoulos et al., 1992) and drive shears of velocity. The spectral properties of magnetic fluctuations from case studies of such types of events suggest a turbulent cascade with a strong anisotropy introduced by the mean magnetic field. The spectral properties of magnetic fluctuations evidence power laws in frequency (in the satellite rest frame) $P(f) \sim f^{-\alpha}$ where $\alpha = 2.6 \pm 0.4$. This value is similar to the observed spectral indices over the kinetic scales in the solar wind or in the magnetosheath. Although the fulfillment of the frozen-in hypothesis over kinetic scales in the plasma sheet is questionable, $\alpha \sim 2.6$ is robustly observed during time intervals of bursty bulk flows. Similar spectral features have been observed during tail current disruption events (Consolini et al., 2005). It is more difficult to observe the scaling features of magnetic fluctuations over the supposedly existing turbulent inertial ranges in the plasma sheet. The available spatial scales where fluctuations can develop depend on the type of turbulence driving mechanisms. For example, when turbulence is driven by reconnection-associated bursty flows, the spatial scales along flow directions can be 15 R_E (Vörös et al., 2007a); however, the transversal scales, in

the direction normal to the flow, are of the order of 2–4 R_E (Nakamura et al., 2004).

The limited dimension of the flow channels together with the flapping motion of the plasma sheet and short duration of the flows (typically several minutes) make it almost impossible to observe the inertial scale fluctuations or use multipoint wave telescope techniques in this region (Pinçon and Lefeuvre, 1991; Motschmann et al., 1996; see also the review by Narita, 2017). There exist as well observations when the spacecraft were constantly in the inner plasma sheet for longer times, like Geotail for seven hours on 25 January 2000. In that instance, bursty flows or groups of flows were observed and for carefully selected stationary subintervals the inertial scale spectral index, $\alpha = 1.8 \pm 0.4$ was clearly observed (Vörös et al., 2007b).

The scaling spectral properties can be consistent with anisotropic models of MHD turbulence proposed for solar wind (Goldreich and Sridhar, 1995; see also Vörös et al., 2004), although, as pointed out by Borovsky and Funsten (2003), some basic hypotheses of this model are violated in the plasma sheet. Interestingly, case studies of BBF events (Wang et al., 2016) also indicate that, while strongly anticorrelated, the magnetic field and density fluctuations (the latter related to compressible turbulence) have similar scaling properties. Intermittency is seen both in density and magnetic field fluctuations by higher order analysis (kurtosis, see, e.g., Wang et al., 2016). Electric field fluctuations at the smallest scales are linked to turbulence and dissipation via kinetic Alfvén waves and current instabilities, including double layers, in the regions of BBFs braking (Stawarz et al., 2015).

Shear flows in the plasma sheet boundary layer may drive turbulence in the plasma sheet (Borovsky and Funsten, 2003), similarly to shear-driven turbulence in the neutral fluids wakes, as illustrated in Figure 5.4 (Gentile et al., 2016). It is supposed that unstable Kelvin–Helmholtz (KH) vortices in the boundary layer (see, e.g., the review by Johnson et al., 2014), possibly related to the nonlinear stage of KH modes, are excited at the magnetopause (Walsh et al., 2015; De Camilis et al., 2016). This mechanism seems plausible; however, no in-depth analysis was performed to test its feasibility for plasma sheet turbulence.

Large-scale plasma sheet vortices leading to turbulence are advocated by Antonova and Ovchinnikov (1999) and Ovchinnikov and Atonova (2017) in relation with the large-scale plasma sheet shear flows and the dawn-dusk electric field. The occurrence of large-scale eddies was confirmed by estimations of the correlation times for magnetic and plasma bulk velocity in the plasma sheet, of the order of approximately 10,000 km from ISEE-2 measurements (Borovsky et al., 1997), and between 4,000 and 10,000 km from Cluster (Weygand et al., 2005; see also Narita, 2016b). Other direct evidence

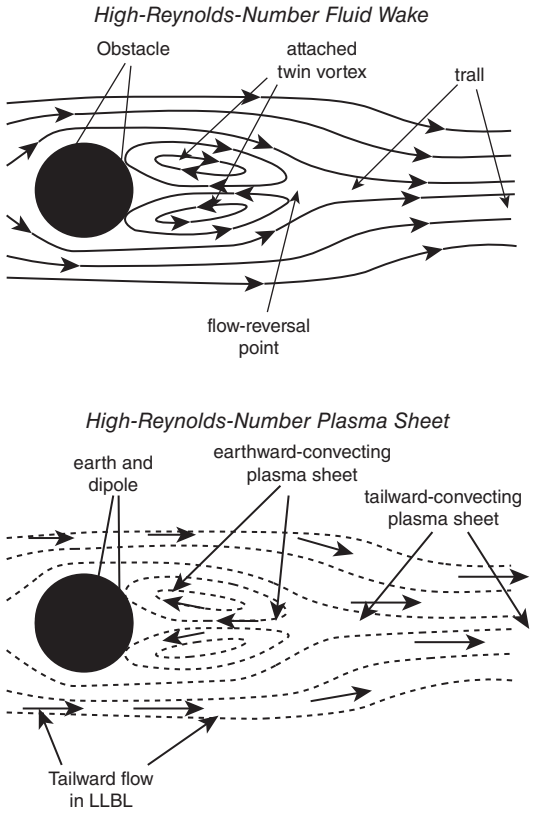

Figure 5.4 High Reynolds plasma sheet turbulence similar to the turbulence in the wake of a neutral fluid flowing past a cylindrical object (from Borovsky and Funsten, 2003)

pointing towards formation of large-scale eddies and related plasma sheet turbulence was provided by auroral imaging and observations of vertical structures and auroral turbulence (Kintner, 1976; Golovchanskaya and Kozelov, 2010; Cousins and Shepherd, 2012). The latter aspect also reveals a fundamental constraint on plasma sheet turbulence (and violation of a key hypothesis for MHD turbulence): the coupling of the plasma sheet with the conducting ionosphere leading to dissipative coupling at virtually all scales (including meso- or inertial range scales). This issue is further discussed in the subsection devoted to dissipation.

Reconnection in the magnetotail is considered to be a source of waves and turbulence (Petkaki et al., 2006; Sergeev et al., 2008). Multispacecraft analysis shows differences between the spectral properties (in the frequency range 0.3–8 Hz) of magnetic fluctuations in tailward and earthward reconnection outflows (Vörös et al., 2008; Narita et al., 2016). Magnetic fluctuations tailward of reconnection seems to show a scale-dependent anisotropy while the anisotropy is strong but virtually scale-independent earthward of reconnection events (Vörös et al., 2008).

It was also conjectured that a magnetohydrodynamic description of the global magnetospheric state allows for emergence of stochastic multiscale coherent structures/states in the tail as a hallmark of "complexity" (Consolini and Chang, 2001; Kretzschmar and Consolini, 2006). In this paradigm, localized reconnections and BBFs in the magnetotail are a natural consequence of the multiscale "complexity" that converts the "configurational free energy" due to nontrivial magnetic configurations into relaxation processes (Hornig and Schindler, 1996; Milovanov et al., 2001). Long-range correlations lead to a scale-free behavior generally recognized as the emergence of power-law scaling also named "criticality" (Kadanoff et al., 1967). The system is also slowly driven out of equilibrium by the continuous interaction with the solar wind while intermittency and turbulence occur as manifestations of a critical-like state (forced and/or self-organized criticality) (Consolini and Chang, 2001; Milovanov et al., 2001). It was demonstrated that the correlation length in the plasma sheet depends on the auroral activity level (Weygand et al., 2010).

Dissipation of Turbulence in the Plasma Sheet and the Magnetotail. Borovsky and Funsten (2003) argued that two mechanisms are important for dissipation of turbulence in the plasma sheet: (1) multiscale electric coupling with the ionosphere and (2) eddy and wave dissipation at high wave numbers. The magnetosphere–ionosphere coupling contributes to dissipation of the plasma sheet turbulence through field-aligned currents connecting the plasma sheet vortices to the resistive ionosphere; this process acts like a kind of viscosity. From geometrical and dimensional analysis Borovsky and Funsten (2003) conjectured that the typical plasma sheet vortices map into elongated auroral structures extending hundreds of kilometers in the azimuthal direction and several kilometers in the North–South direction, respectively. The power dissipation rate ranges between 7×10^5 and 10^7 W and dissipation times take values between 70 and 1,300 seconds (Borovsky and Funsten, 2003). This dissipative coupling with the ionosphere adds additional complications to treating turbulence in the plasma sheet, as the dissipation depends on the size of the eddies. It also manifests at all wave numbers, to be contrasted with the homogeneous MHD inertial range of scales that is clearly separated from dissipation scales and is dominated by the nonlinear transfer of energy (or cascade), as illustrated by diagrams in Figure 5.5. In other words, the dissipative coupling with the ionosphere may inhibit the forward cascade postulated for the inertial range homogeneous MHD turbulence. Simulation studies indicate that reconnection associated outflows are sources of significant free energy that can drive instabilities and lead to additional dissipation and energy conversion (Lapenta et al., 2018).

At higher wave numbers the dissipation shows features similar to solar wind turbulence (see, e.g. Vörös et al., 2008). Indeed it is advocated that thin current sheets are sites of small-scale reconnections that dissipate energy (Matthaeus and Lamkin, 1986; Leamon et al., 2010; Loureiro and Boldyrev, 2017). The role of Landau damping is also recognized (Leamon et al., 1998). However, due to the prominence of eddy versus Alfvén turbulence in the plasma sheet and to the dissipative coupling to the ionosphere the role of cyclotron interactions with ions and electron is believed to be of less importance (Borovsky and Funsten, 2003). Magnetic reconnection in the plasma sheet appears to be associated with magnetic turbulence, wave activity, enhanced current densities, and parallel electric fields. The electric field can play a key role in turbulent dissipation and particle acceleration in the magnetotail (Ergun et al., 2018).

The current sheet instabilities at the interface between coherent structures leading to their collapse and mutual merging contribute to a coarse-graining dissipation and/

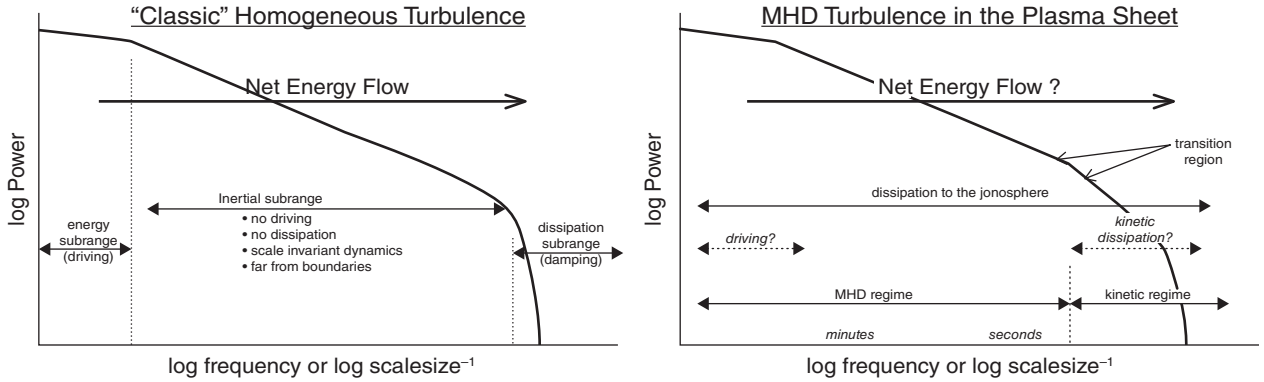

Figure 5.5 Diagrams of homogeneous MHD turbulence (left) and plasma sheet turbulence (right). Diagram from Borovsky and Funsten (2003).

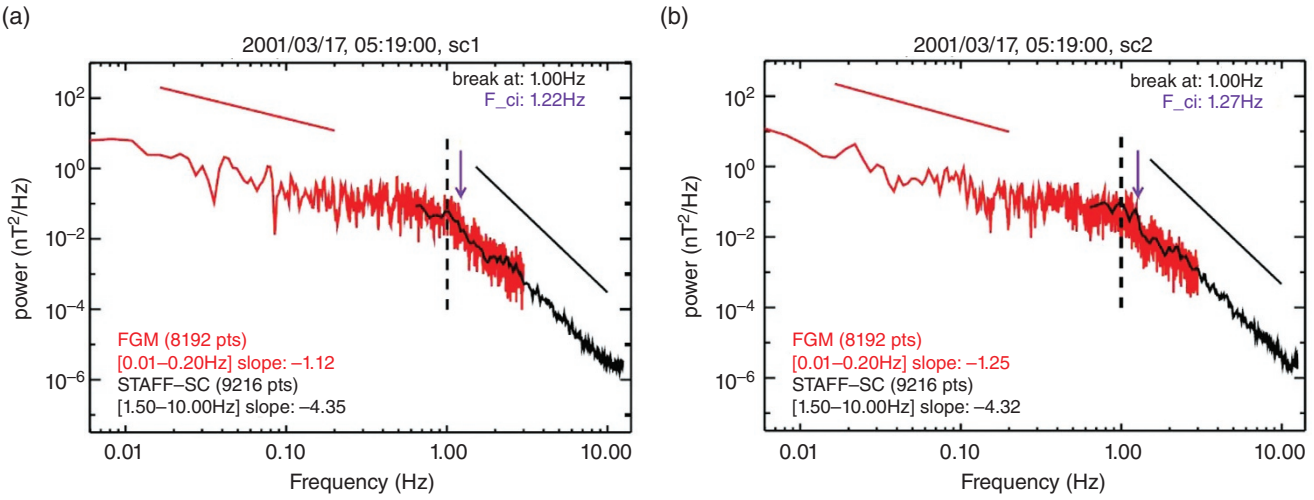

Figure 5.6 Examples of total power spectral densities (trace of the power spectral matrix) computed from magnetic field measurements by Cluster in the terrestrial cusp. Red profiles identify data from the fluxgate instrument; black lines indicate data from wave analyzer. The two panels correspond to data from two of the four Cluster spacecraft. The arrow indicates the ion cyclotron frequency and the dashed line indicates the spectral break. Figure published by Nykyri et al. (2006).

or inverse cascade due to the medium-sized eddies merging and thus transferring energy to the resulting larger and smaller scale eddies (Wu and Chang, 2001; Chang et al., 2004). (A detailed example of coarse-grained dissipation at MHD scales may be found in section 3.6 of the book, *An Introduction to Space Plasma Complexity*, by Chang, 2015.) High resolution kinetic numerical simulations reveal that coherent structures of this type indeed form in two-dimensional turbulent plasma where they mutually interact (Servidio et al., 2012). As conjectured by Chang et al. (2004) the dynamical complexity of such structures leads to involved spatiotemporal behavior, including those in the phase space (see, e.g., Valentini et al., 2014). Possible hints pointing towards a dynamical complexity of the plasma sheet turbulence were provided by multipoint analysis of higher order moments of magnetic field fluctuations recorded by Cluster (Weygand et al., 2005).

5.3.3. Auroral and Cusp Regions – Sites of Turbulence and Plasma Complexity

The plasma and field fluctuations observed in the magnetospheric cusps and the auroral regions are perhaps the best illustration of the complex and turbulent dynamics of a driven space plasma system. Intermittency and sporadic intense dissipation events are dominant in these regions. Therefore, a description of turbulence in terms of classical concepts is not fully justified. This section is devoted to a discussion of experimental observations of turbulence in the cusp and auroral regions and an introduction to modern analysis methods for magnetospheric turbulence/complexity, such as wavelets, probability distribution functions, and multifractals, with emphasis on a relatively new technique, successfully employed for the complexity phenomena in these regions, the Rank Ordered Multifractal Analysis (ROMA).

Dynamics of Turbulence in the Cusp. The same arguments put forward when discussing the dynamics of turbulence in the magnetospheric tail may be invoked for the cusp turbulence. Indeed, the cusp, a region populated by shocked solar wind, is limited to a funnel-shaped structure above the two magnetic poles whose inner boundary is the magnetopause (Heikkila and Winningham, 1971). Its spatial dimension is less than two orders of magnitude larger than the kinetic (dissipative) ion scales that can impede the formation of a proper inertial range of turbulence. Nevertheless, multipoint observations of magnetic and electric field fluctuations in the cusp reveal Kolmogorov-like scaling of Power Spectral Density ($f^{-1.7}$) with a spectral break marking the transition to steeper scaling ($f^{-2.8}$) around the local proton gyrofrequency (Nykyri et al., 2006; Wang et al., 2014) (Figure 5.6). Furthermore, some studies suggest that the exterior cusp may however take the form of a spatially extended region spanning between 4.5 and 9 R_E along the magnetopause with a typical cross dimension of the order of 1.3 R_E (Walsh et al., 2012).

The cusp is also the site of strong plasma waves spanning a broad range of frequencies, from ion cyclotron to electron whistlers and kinetic Alfvén waves (Pickett et al., 2001; Khotyaintsev et al., 2004; Wang et al.,

2014). Whether these waves are part of a cusp turbulence in the classical sense of the term is not clear (see the discussion by Nykyri et al., 2011). An important feature revealed experimentally by missions like Interball and Polar is the so called Cusp Turbulent Boundary Layer, a distinct region of a characteristic size of 300–5,000 km, just outside the magnetopause on the cusp side (Savin et al., 1998, 2002; Pickett et al., 2001) that can, at times, occupy parcels on the magnetospheric side of the cusp magnetopause (Dubinin et al., 2002). This layer is a site of intense magnetic and electrostatic turbulent wave activity (Pickett et al., 2001). The presence of eddies/vortices, small-scale current sheets and other coherent plasma structures in the cusp and its turbulent boundary layer is also confirmed (Sundkvist et al., 2005; Nykyri et al., 2011).

Driving of Turbulence in the Cusp. The existence of electromagnetic fluctuations and turbulence in the cusp raise questions on the driving mechanisms. Several scenarios can be considered: (1) small-scale magnetic vortices (-Sundkvist et al., 2005), (2) velocity shears of ion beams (Lakhina, 1990), (3) local transport of magnetosheath material from localized reconnection/merging events (Dubinin et al., 2002) or direct entry of solar wind plasma (Lundin and Dubinin, 1985; Woch and Lundin, 1992). Nevertheless, there are no studies devoted to an in-depth investigation of these mechanisms and a critical comparison.

Small-scale magnetic vortices were detected from multipoint observations by Cluster in the cusp and are characterized by spatial scales of the order of several proton Larmor radii, roughly several tens of kilometers (Sundkvist et al., 2005). It is believed they are fundamental plasma modes resulting from the self-organization and nonlinear interaction of obliquely propagating drift and kinetic Alfvén waves driven by sheared plasma flows (see also, Shukla et al., 1986; Liu and Horton, 1986). These structures bear similarities with the Alfvénic vortices advocated for the magnetosheath (Alexandrova, 2008) and pertain perhaps to the same class of phenomena. Although they can span an enlarged domain of scales, is not likely that this type of structure can sustain a nonlinear cascade leading to power-law scaling observed in the inertial range.

It was shown, from theoretical arguments, that cold and hot ion beams with velocity shears along cusp magnetic field lines excite resonant and nonresonant kinetic Alfvén mode instabilities (Lakhina, 1990). A relatively broad spectrum of waves is indeed observed in connection to counterstreaming magnetosheath ions flowing along cusp magnetic field lines (Le et al., 2001; Grison et al., 2005). Multispacecraft observations from Cluster allowed identification of kinetic Alfvén waves as a dominant mode during ion injection events (Grison et al., 2005). However, observations also show that the magnetic power spectral densities obtained during ion beam events exhibit outstanding prominent spectral peaks (Le et al., 2001) that are inconsistent with the standard picture of turbulent energy cascade characterized by a power law. Thus the ion beams seem to be more related to the occurrence of wave emission than to a proper turbulent topology. Moreover, some of the ion injections might be manifestations of entry events discussed in the next paragraph.

Most of the time, however, the cusp is populated by magnetosheath plasma. The advocated entry mechanisms rely on magnetic merging/reconnection (Dubinin et al., 2002) or direct/impulsive penetration (Lundin and Dubinin, 1985; Woch and Lundin, 1992; see also Echim and Lemaire, 2000). Regardless the type of the entry mechanism, the magnetosheath plasma "carries" its turbulent properties, possibly linked to the turbulent state at the origin, in the solar wind. This might possibly explain the Kolmogorov-like spectra observed at times in the cusp (Nykyri et al., 2006; Wang et al., 2014) which would be a "remnant" of solar wind turbulence. At least part of the solar wind nonlinear cascade topology, i.e. the eddies at scales smaller than cusp's typical size, might survive the traversal of the bow shock and they could continue to "actively" contribute to the nonlinear transfer of energy through scales. However, the presence of regions of stagnant magnetosheath plasma in the cusp (Dubinin et al., 2002) indicates the (partial) evanescence of turbulence in the cusp during entry events.

Dissipation of Turbulent Energy in the Cusp. Since the main characteristics of plasma in the cusp are similar to solar wind and the magnetopsheric environment one would expect the physical mechanisms for dissipation of turbulent energy to be similar. Multipoint observations of magnetic field fluctuations in the cusp allowed estimation of the wave structure in the k-space and identified kinetic Alfvén waves in the frequency domain at scales around and smaller than the ion Larmor radius, corresponding to the spectral break (Wang et al., 2014). The origin of these waves was assigned to density gradients through a resonance-convergence mechanism at the interface between the cusp and the magnetosheath. However, the damping of these waves in the frequency range typical for ion kinetic range was moderate (Wang et al., 2014), contrary to reports of kinetic Alfvén wave (KAW) damping in the solar wind (Sahraoui et al., 2010). Nevertheless, the damping through electron Landau damping of KAW was not probed for the cusp turbulent dissipation. Nykyri et al. (2006) discussed damping of additional modes and found that ion cyclotron modes with all angles of propagation are efficiently damped while damping of magnetosonic and of ion Bernstein modes is negligible.

Intermittency Analysis of Electrostatic Fluctuations in the Auroral Zone. Let us now turn our attention to additional interpretations of the observed fluctuations in the auroral regions and introduce additional data analysis strategies that allow understanding the structure of these fluctuations, particularly of their intermittent features. The origin of intermittent fluctuations in magnetized plasmas may also be interpreted as the result of the sporadic mixing and/or interactions of localized pseudo coherent structures interspersed with energy carrying propagating waves.

The dominant forms of such structures in the auroral zone are the pseudo 2-D oblique potential structures. The interactions of these structures are the manifestation of localized reconnections/mergings mediated by intermittent inertial Alfvén waves, fractions of other electrostatic and electromagnetic fluctuations, generalized resistivity, and coarse-grained dissipation (Chang, 2001). Thus, one expects a significant fraction of such fluctuations to be electrostatic and transverse. When detected in the spacecraft (rocket) frame, the signatures of these fluctuations are Doppler shifted and have relatively slow moving speeds in the rest frame interspersed with small components of electrostatic and/or electromagnetic waves.

As an example, we consider below the intermittency of the Broadband Extremely Low Frequency (BB-ELF) electric field fluctuations in the auroral zone, as measured by the Sounding of the Ion Energization Region: Resolving Ambiguities (SIERRA) rocket mission (Tam et al., 2005). Results of the data analyses are discussed based on techniques like wavelet analysis, local intermittency measure (*LIM*), and Flatness. Figure 5.7(top) shows typical electric field fluctuations, normal to the auroral magnetic field, E_{north}. By averaging over 1,910 spectra, the spectral density within a special time interval is calculated. Figure 5.7 (bottom) indicates the fluctuations are broadband in nature, with a power-law spectral density covering the extremely low-frequency range (3–200 Hz) within the auroral region.

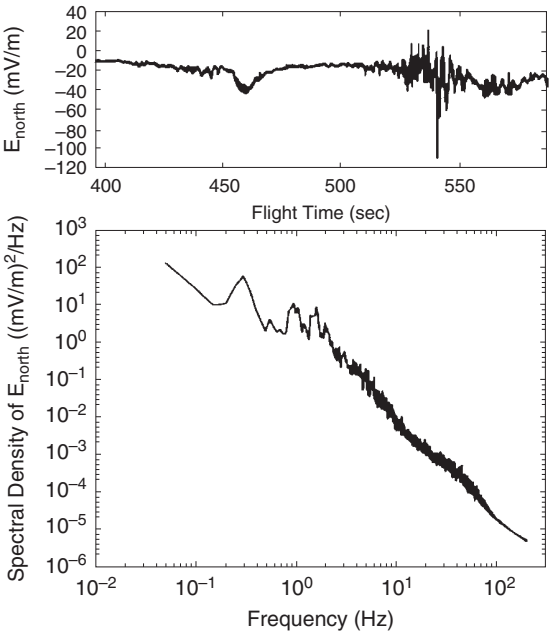

Figure 5.7 Top: typical electric field fluctuation component normal to the auroral magnetic field, E_{north}. Bottom: spectral density within a special time interval (averaged over 1910 spectra) (from Tam et al., 2005).

Intermittent fluctuations may be analyzed using wavelet transforms that generally are composed of modes that are square integrable localized functions capable of unfolding fluctuating fields into time (or space) and scales. To study the intermittency of fluctuations at different scales, we define the Local Intermittency Measure (*LIM*): $LIM(s,t) = |W_s(t)|^2/\langle|W_s(t)|^2\rangle_t$, where $W_s(t)$ are the wavelet coefficients at various scale s and time t (Farge, 1991; Kovacs et al., 2001). Based on the Haar wavelet transform (Bruno et al., 2001), an example of a map of *LIM* computed for fluctuations of the E_{north} component of the electric field measured by the SIERRA experiment in the auroral regions is shown in Figure 5.8. The spectral power of the fluctuations mainly concentrates at scales of 320 ms or larger and the *LIM* analysis indicates that the power of intermittent events is generally larger at small scales.

A direct measure of the degree of intermittency is related to the fourth-order moment of the probability distribution function (see the discussion in the next section) through the so-called flatness parameter:$F(s) \equiv \langle[LIM(s,t)]^2\rangle$. We note that for Gaussian fluctuations, $F = 3$. Figure 5.9 shows the flatness for E_{north} (based on the Haar wavelets), recorded by the SIERRA experiment. At small scales, the flatness varies inversely with the time scale. At scales of few milliseconds, the flatness increases to several thousands, verifying strong intermittency of fluctuations at small scales.

Using the observed turbulent fluctuations, it will be possible to calculate the global energization and acceleration of charged particles and their phase space

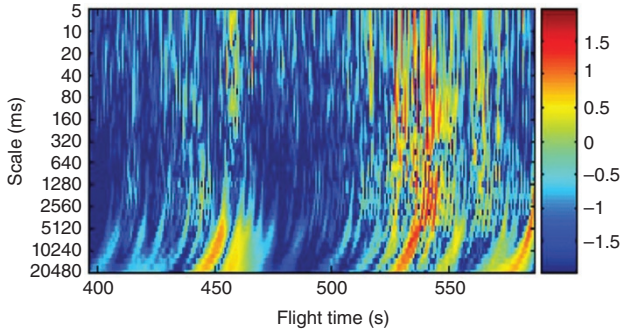

Figure 5.8 Local intermittency measure (LIM) for E_{north} (from Tam et al., 2005).

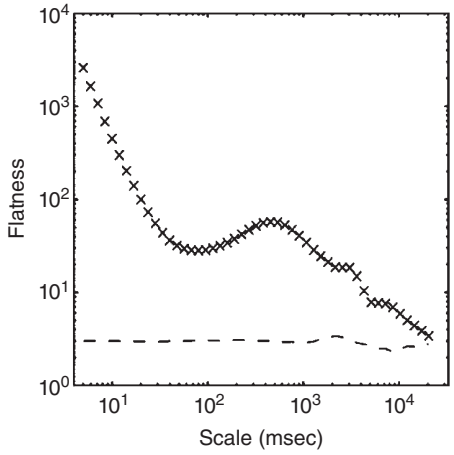

Figure 5.9 Flatness for E_{north} (from Tam et al. 2005).

distributions using kinetic and/or fluid equations self-consistently within the auroral range (Chang et al., 2004; Jasperse et al, 2006a, 2006b). Such calculations are, however, too detailed and complicated for inclusion in this brief chapter.

Probabilistic Description of Turbulence and Complexity with Structure Functions and multifractals. The structure of magnetic field fluctuations in the cusp, and particularly their intermittency, was unfolded by higher-order analyses like probability distribution functions, structure functions and multifractals (Yordanova et al, 2004, 2005; Echim et al., 2007). Let us briefly introduce this methodology and consider a generic time series of a certain physical turbulent measure: $\mu(t)$. The discussions in the next few sections apply equally well for temporal series/scales τ and spatial measures/scales δ. To address its fluctuating characteristics, we may form the scale-dependent difference series $\delta\mu = \mu\,(t + \tau) - \mu\,(t)$ and consider the normalized histograms of differences $\delta\mu$ at scale τ, i.e. the probability distribution functions (PDFs) $P(\delta\mu, \tau)$ for a range of temporal scales τ. Such PDFs for turbulent variables are generally non-Gaussian with extended tails for intermittent fluctuations. An example of non-Gaussian PDFs computed for cusp magnetic field fluctuations measured by the four Cluster spacecraft is shown in Figure 5.10 (Echim et al., 2007).

To study the phenomenon of intermittency we may consider the structure functions, S_q, defined as the moments of order q of the PDFs: $S_q\,(\delta\mu, \tau) = \int (\delta\mu)^q P(\delta\mu, \tau) d(\delta\mu)$. The motivation here is that different moments q emphasize different peaks in the fluctuating series. Generally, corresponding to each S_q one defines a fractal (structure function) exponent ζ_q that satisfies the power law relation $S_q = \tau^{\zeta_q}$ for some limited range of small values of τ.

When the scaling exponent ζ_q varies linearly with the moment order q, the fluctuating variable in that range of scales (and the dynamical process at the origin of these fluctuations) is considered monofractal or self-similar. When the linear relation between ζ_q and q is not satisfied, the fluctuating phenomenon is considered multifractal. An example of multifractal behavior of cusp magnetic fluctuations is shown in Figure 5.11 (Yordanova et al., 2004). The right-hand panel of this figure shows the scaling exponents evaluated by a linear least-squares fit to the double logarithmic plot, log S_q versus log Δt, and using the formula $\tau(q) = \zeta_q - 1$; the figure also shows the scaling exponent derived from an alternative approach based on the wavelet transform modulus maxima (WTMM) (Mallat and Zhong, 1992).

The probabilistic analysis of cusp data identified an extended range of scales where PDFs are non-Gaussian compared to the PDFs computed in the magnetosheath (Echim et al., 2007). The structure function and multifractal analysis of cusp magnetic fluctuations also revealed anisotropic behavior: the magnetic fluctuations parallel to the main field can be described by a self-similar, monofractal process while the perpendicular fluctuations are characterized by a strong intermittency with multifractal topology (Yordanova et al., 2005). These findings suggest the plasma dynamics in the cusp can be understood in terms of dynamical coherent stochastic structures forming a complex medium consisting of a hierarchy of multiscale interacting dynamical structures. In the following a mathematical apparatus developed specifically for such complex dynamical systems is discussed.

Rank-Ordered Multifractal Analysis (ROMA). Because the conventional structure function formalism is based on the moments of the full set of fluctuations (which are dominated by those of the small amplitudes), the physical interpretation of the multifractal nature is not easily deciphered by merely examining the curvatures of the deviations from linearity. Furthermore, the structure function exponents are poorly defined because rarely do the actual data exhibit truly power-law relationships between S_q and τ over the entire scaling range. In addition, even though structure function calculations may be performed conveniently for a fluctuating series for positive values of q, they invariably exhibit divergent characteristics for $q < 0$.

It appears then reasonable to search for a procedure that explores the fractal, i.e. power-law scaling behavior of the subdominant fluctuations by first appropriately isolating out the minority populations and then performing the statistical investigation for each of the isolated populations. Such grouping of fluctuations must depend somehow on the sizes of the fluctuations. However, the groupings cannot depend merely on the raw values

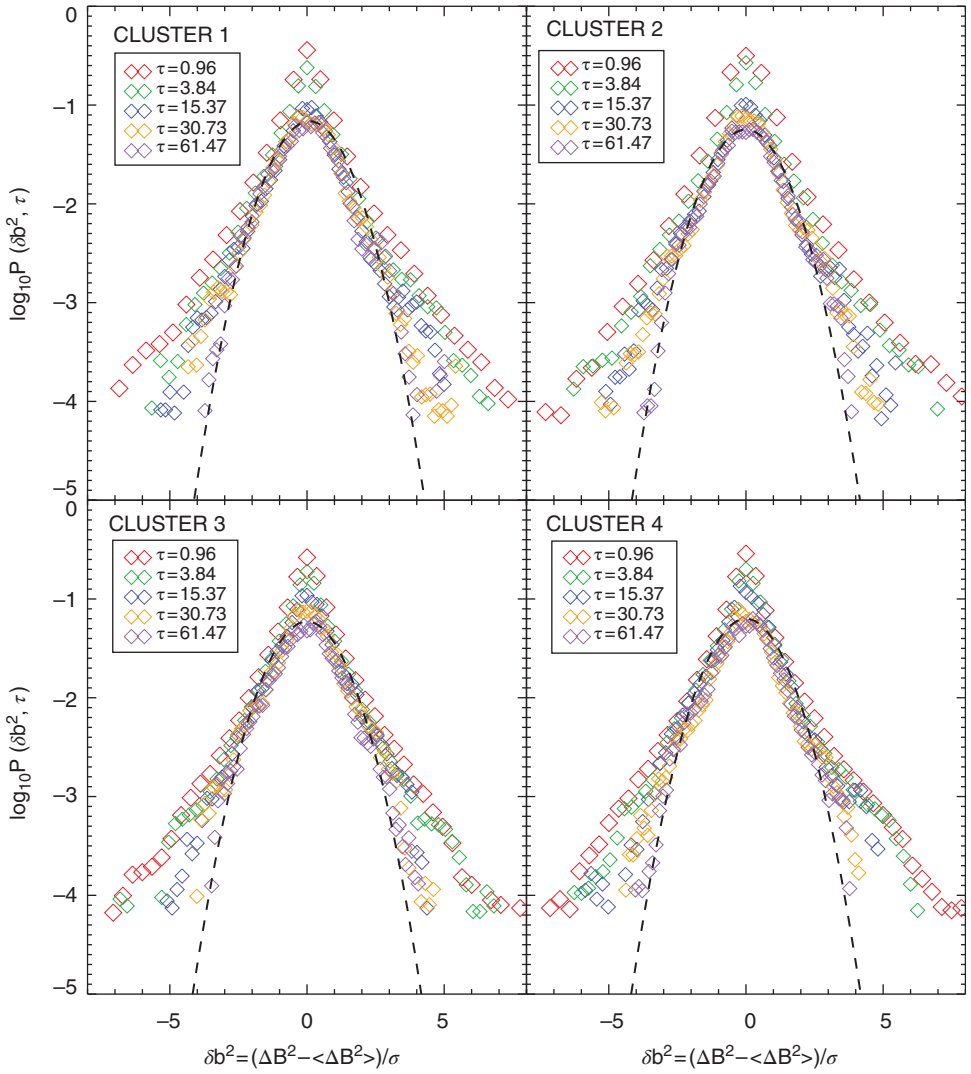

Figure 5.10 Probability Distribution Functions (PDFs) of fluctuations measured in the terrestrial cusp by the four Cluster spacecraft. The dashed lines correspond to Gaussian functions and illustrate the departure from Gaussianity at virtually all illustrated scales (from Echim et al., 2007).

of the sizes of the fluctuations because the ranges of the fluctuating sizes will be different for different scales. Therefore, we are led to proceed to rank-order the sizes of the fluctuations based on the local fractal invariant $Y = \delta\mu/\tau^s$, where s is the scaling exponent for each (local) grouping.

Consider a differential range of dY in the vicinity of some scaled size $Y = \delta\mu/\tau^s$. We expect the fluctuations whose sizes fall within this differential range to exhibit monofractal behavior characterized by the local scaling exponent s such that the differential structure function dS_q will vary with the scale as τ^{sq} according to:

$$dS_q = (\delta\mu)^q P(\delta\mu, \tau) d(\delta\mu) = \tau^{sq} Y^q P_s(Y) dY \qquad (5.1)$$

Given an ensemble of PDFs $P(\delta\mu, \tau)$, the corresponding multifractal spectrum $s(Y)$ may be obtained approximately (if the ansatz is valid) by integrating the functional differential expression (5.1) over small contiguous ranges of ΔY with the assumption that within each incremental range the scaling exponent s is essentially a constant. Thus, for a range of ΔY within (Y_1, Y_2), we form a range-limited structure function as follows:

$$\Delta S_q(\delta\mu, \tau) = \int_{a_1}^{a_2} (\delta\mu)^q P(\delta\mu, \tau) d(\delta\mu) = \tau^{sq} \int_{Y_1}^{Y_2} Y^q P_s(Y) dY \qquad (5.2)$$

where $a_1 = Y_1\tau^s$ and $a_2 = Y_2\tau^s$. We may then search for the value of s such that the scaling property of the range-limited structure function that varies with s is: $\Delta S_q(\delta\mu, \tau) = \tau^{sq}$. If such a value of s exists, then we have found one region of the multifractal spectrum of the fluctuations such that the PDFs in the range of ΔY collapses onto one scaled

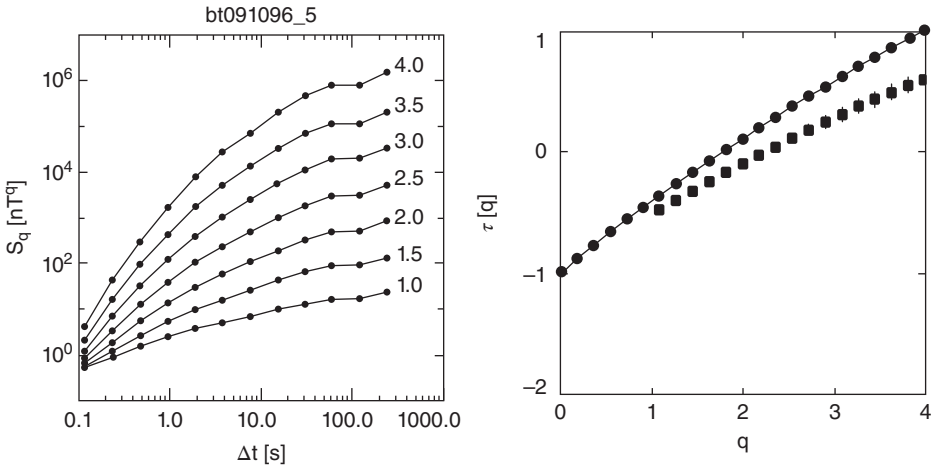

Figure 5.11 Left: structure functions of magnetic field fluctuations recorded in the auroral regions by the Polar spacecraft (Yordanova et al., 2004); the figure shows S_q as a function of scale Δt for seven different orders: $q \in [1, 1.5, 2, 2.5, 3, 3.5, 4]$ and temporal scales between 0.1 and 1000 seconds. Right: scaling exponents $\tau(q)$ as a function of the moment order q computed with WTMM (circles) and the least square fit of log S_q as function of log Δt (squares), where $\tau(q) = \zeta_q - 1$. The two figures are published by Yordanova et al. (2004). The nonlinear change of the scaling exponent with the moment order q indicates a multifractal structure of magnetic field fluctuations.

PDF. Performing this procedure for all contiguous ranges of ΔY will produce the approximate rank-ordered multifractal spectrum $s(Y)$ that we are looking for.

The determined value of s for each grouping should be unaffected by the statistics of other subsets of fluctuations that are not within the chosen range ΔY and therefore should be quantitatively quite accurate. If this spectrum exists, the PDFs for all time lags collapse onto one master multifractal scaled PDF, $P_s(Y)$. The spectrum will be implicit since Y is defined as a function of s (the local Hurst exponent). The above procedure, commonly known as ROMA (rank-ordered multifractal analysis), was first introduced by Chang and Wu in 2008.

We illustrate the procedure discussed above based on magnetic field records observed by the four Cluster spacecraft during a long crossing of the Northern cusp (Echim et al., 2007). Prior to the fractal analysis an implicit partial removal of the dipole component of the magnetic field fluctuation is achieved by computing first the differences $\delta B^2(t, \tau)$ from the raw data with τ being the time scale and then the mean value of the fluctuations at each scale is subtracted yielding a new "ensemble" of fluctuations (Echim et al., 2007)

$$\delta b^2 \equiv \frac{\delta B^2(t,\tau) - \langle \delta B^2(t,\tau) \rangle}{\sigma^2} \tag{5.3}$$

where the bracket indicates the ensemble average and σ is the variance. Typical PDFs were computed for the quantity, δb^2, where differences δB^2 have been calculated by moving an overlapping window of width $\tau = 2^j \delta t$ over the entire time interval with $\delta t = 0.0015$ seconds being the time resolution of the measurements and $j = 1, 2, \ldots, 15$, as shown in Figure 5.10. In this analysis, we shall adopt the Taylor hypothesis (1938), which assumes the temporal fluctuations observed in satellite data correspond to spatial fluctuations.

A ROMA analysis using the aforementioned approximate integral technique was performed for the chosen data set in the cusp region (Chang et al., 2010; Chang, 2015) and the results are shown in Figure 5.12. We note that for small Y, the fluctuations were persistent ($s > 0.5$), indicating the turbulence was unstable and probably not yet completely fully developed. For larger values of Y, the fluctuations became antipersistent ($s < 0.5$) and sparser and sparser as the value of Y increased. (The special situation for $s = 0.5$ may be shown to correspond to fluctuations of classical random diffusion.) The ROMA spectra for all four spacecraft were very similar; indicating that despite the magnetic field fluctuations were anisotropic, the magnetic energy density fluctuations in the cusp were essentially statistically isotropic over the distance covered by the cusp passage for spatial scales of the separation distance between the Cluster spacecraft (~1,000 km).

Comparison with ROMA of Solar Wind Turbulence. We compare the above cusp results with solar wind turbulence based on a particular set of WIND data (Chang et al., 2008). The solar wind ROMA spectrum presented in Figure 5.13 has the similar signature of Figure 5.12. However, it is much flatter with the range of the fractal index s lying between 0.44 and 0.38. The turbulence is antipersistent, fully developed, and essentially monofractal. Thus, the observed PDFs collapse nearly onto one single curve for $s = 0.44$ as shown by Figure 5.14. A quite

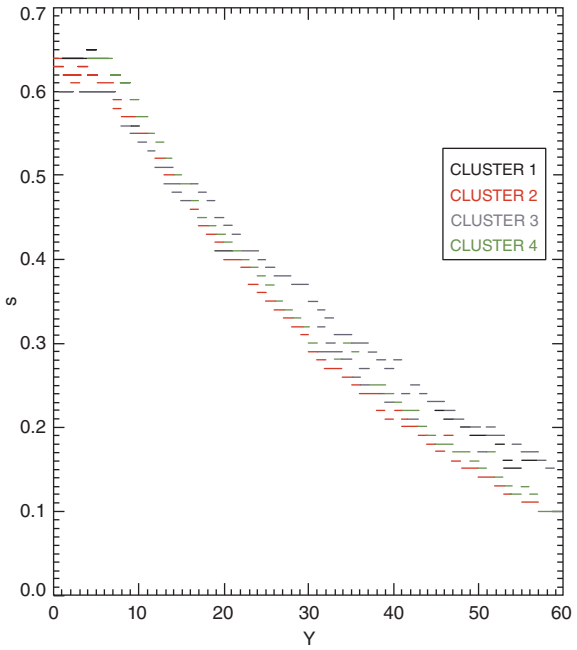

Figure 5.12 ROMA spectra for magnetic field fluctuations recorded in the cusp by the four Cluster spacecraft (from Chang et al., 2010).

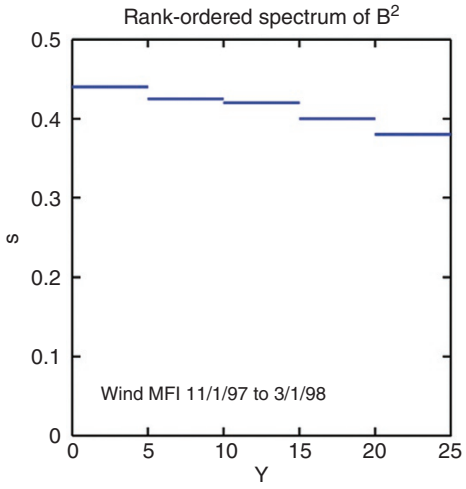

Figure 5.13 Rank-ordered multifractal spectrum for a particular set of solar wind data from WIND for fluctuations between 3 and 1,500 seconds. The spectrum is calculated for five contiguous ranges of ΔY. Figure published by Chang et al. (2008).

similar result was obtained by Hnat et al. (2002) for another set of WIND data.

Double Rank-Ordering of BB-ELF ROMA – Crossover from Kinetic to MHD Scales. We now demonstrate the crossover phenomena of ROMA scaling based on the

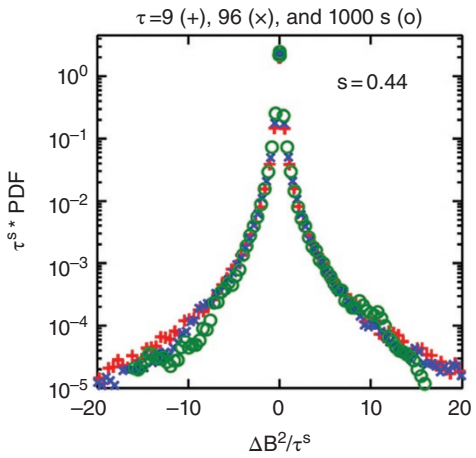

Figure 5.14 Scaled PDFs for the solar wind data of Figure 5.13 (figure published by Chang et al., 2008).

auroral rocket data discussed in the earlier part of this section (Tam et al., 2010, 2011). Since the dominant fraction of the electric field variations in the observational region were known to be nearly nonpropagating intermittent turbulence composed mainly of multiple interacting inertial Alfvénic potential structures, the observed time series were interpreted in terms of spatial fluctuations with $\Delta \approx U\tau$, where $U \approx 1.5$ km s^{-1} is the horizontal speed of the rocket, τ the time scale and Δ the corresponding spatial scale.

In analyzing the data, it was discovered that the observed fluctuations span across four contiguous regimes of scales (from kinetic to inertial Alfvénic, to intermediate, and eventually to the MHD scales) with different multifractal characteristics. A rank ordered multifractal spectrum was found for each regime: $s_1(Y_1)$ for kinetic range, $s_2(Y_2)$ for inertial Alfvénic, $s_3(Y_3)$ for intermediate and $s_4(Y_4)$ for MHD range of scales (see Figure 5.15, top panel). The dividing times between the adjacent regimes were determined to be roughly $\tau \approx 80$ ms, $\tau \approx 160$ ms, and $\tau \approx 320$ ms.

Thus, the observed intermittent turbulence of the auroral electric field fluctuations was found to be characterized by two rank-ordered parameters: the index i and the power-law scaling variable Y_i. Assuming the nonlinear crossover regions between the adjacent regimes were narrow, the ROMA spectra were mapped onto one global scaling variable with a single global scaling function (Figure 5.15, bottom panel). Such a mapping served the purpose of demonstrating the ROMA spectrum as multivalued and provided a convenient display of the individual multifractal characteristics for each rank-ordered index i. It also demonstrated the generalization of the idea of monofractal mapping to the concept of multiparameter mapping involving crossover effects among multifractals.

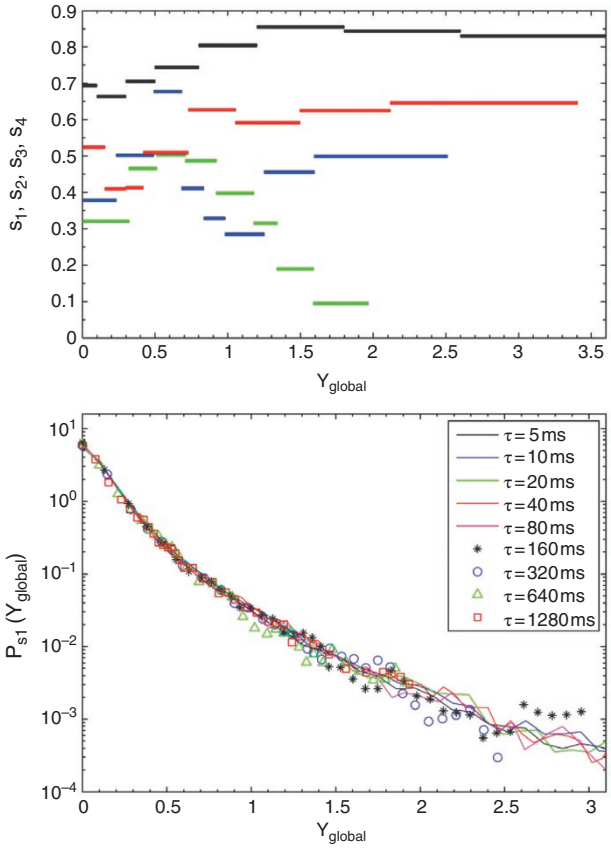

Figure 5.15 Top: rank-ordered spectra s_1 (black), s_2 (red), s_3 (blue), and s_4 (green) over the ranges of Y_{global}. Bottom: global scaling function $P_{s1}(Y_{global})$ obtained from the PDFs at all the time scales of the four regimes (from Tam et al., 2010).

5.4. SUMMARY AND OUTLOOK

In this chapter some key facts about turbulence and complexity in the terrestrial magnetosphere have been reviewed, focusing on three main magnetospheric subsystems: (1) the magnetosheath, (2) the tail/plasma sheet, and (3) the cusps/auroral regions. While in the solar wind the turbulence is freely decaying and the boundaries play a minor role in the development of turbulence, the magnetospheric context is fundamentally different; the key regions are bounded and have fundamentally different physical characteristics with deep impact on turbulence properties. Each magnetospheric region is unique and the data show a broad range of conditions and manifestations of turbulence and complexity. We attempted to discuss the still unsolved issues and present the reader a list of research topics that await further investigations/clarifications.

The terrestrial magnetosheath, at the interface with the solar wind, raises puzzling questions regarding its turbulent state. The magnetosheath is a bounded system, confined between the bow shock and the magnetopause; therefore, the turbulence might not be fully developed. The anisotropy and the geometry of the upstream bow shock play an important role for the plasma dynamics and excitation of waves and instabilities. Waves, like the mirror mode and the Alfvén ion cyclotron mode, play a role in relaxing the temperature anisotropy and leading to fluctuations and turbulence. However, experimental observations provide evidence for the occurrence of nonlinear structures, like the Alfvén vortices, possibly linked to spectral properties of magnetosheath fluctuations otherwise not explained by the linear theory. Recent studies provide evidence for a lack of a proper inertial-like scaling for ranges of scales, at distances closer to the bow shock. Some interpretations consider this behavior possibly a signature of the "destructuring" of the solar wind turbulence at the bow shock accompanied by creation of new structures and fluctuations that inhibit the formation of an energy cascade. This is a field of research that requires further analyses and missions like MMS can certainly contribute in this respect.

The magnetotail and the plasma sheet are also bounded regions: the ionosphere represents the inner boundary while the magnetopause plays the role of the outer one. It is argued that the typical spatial scale of the magnetotail and plasma sheet does not truly allow for a good separation between the dissipation and the driving scales, thus the fundamental hypothesis of MHD turbulence is not satisfied. The type of dynamics leading to turbulence is not fully understood: the physical characteristics of the magnetotail and plasma sheet point towards a type of turbulence similar to the one observed in channels populated by high Reynolds number fluids. There is evidence that the magnetotail turbulence is dominated by eddies (two-dimensional turbulence) rather than Alfvén waves (slab turbulence). The driving of plasma sheet turbulence is not fully elucidated, several mechanisms are considered of importance: bursty bulk flows (BBFs), low-latitude-boundary-layer sheared flow, shears in large-scale tail flow, turbulent and sporadic reconnections, and global reorganization of the plasma sheet state as in critical phase transitions. In the magnetotail and plasma sheet, dissipation is an open question. Numerical simulations suggest that current instabilities can play an important role. On the other hand the coupling with the conducting ionosphere adds a level of complexity, as this coupling manifests itself over a broad range of scales leading to dissipation of energy at virtually all scales – an additional violation of the fundamental hypothesis of classical MHD turbulence.

The magnetospheric cusps are perhaps the example that illustrates best the complexity of plasma dynamics in the terrestrial environment. The probabilistic description of electric field and magnetic field fluctuations shows

properties that evidence complex topologies, dominated by intermittency and non self-similar behavior. New analysis tools are developed, like the rank-ordered multifractal analysis (ROMA) applied for the analysis of MHD space plasma turbulence and also in other astrophysical contexts. It is found that in the cusps the energy transfer rate is nonuniform and highly fragmented consistent with the multifractal topology.

ACKNOWLEDGMENTS

The authors acknowledge support from the European Commission Framework 7 programme through project "Solar system plasma turbulence: observations, intermittency and multifractals – STORM."

ME acknowledges support from the Belgian Solar Terrestrial Center of Excellence (STCE) as well as the Romanian UEFISCDI PCCDI 789 Project VESS and Program Nucleu LAPLAS-ISS.

GC was financially supported by the Italian MIUR-PRIN grant 2017APKP7T on "Circumterrestrial Environment: Impact of Sun–Earth Interaction".

EY was funded by the Swedish Contingency Agency, grant 2016-2022.

ZV was financially supported by the Austrian Science Fund (FWF) under contract P28764-N27.

PK acknowledges the support offered by the ESA project EPHEMERIS (contract No.: 4000128162/19/I-DT).

REFERENCES

Alberti, T., Consolini, G., Carbone, V., Yordanova, E., Marcuci, M.F., and De Michelis, P. (2019), Multifractal and chaotic properties of solar wind at MHD and kinetic domains: An Empirical Mode Decomposition approach, *Entropy*, 21, 320, doi:10.3390/e21030320.

Alexandrova, O. (2008), Solar wind vs magnetosheath turbulence and Alfvén vortices, *Nonlin. Processes Geophys.*, 15 (1), 95–108, doi: /10.5194/npg-15-95-2008

Alexandrova, O., Mangeney, A., Maksimovic, M., Lacombe, C., Cornilleau-Wehrlin, N., Lucek, E. A., et al. (2004), Cluster observations of finite amplitude Alfvén waves and small-scale magnetic filaments downstream of a quasi-perpendicular shock, *J. Geophys. Res.: Space Phys.*, 109, A05207, doi:10.1029/2003JA010056.

Alexandrova, O., Mangeney, A., Maksimovic, M., Cornilleau-Wehrlin, N., Bosqued, J.-M., André, M. (2006), Alfvén vortex filaments observed in magnetosheath downstream of a quasi-perpendicular bow shock, *J. Geophys. Res.: Space Phys.*, 111 (A12), A12208.

Alexandrova, O., Carbone, V., Veltri, P., Sorriso-Valvo, L. (2007), Solar wind Cluster observations: Turbulent spectrum and role of Hall effect, *Planet. Space Sci.*, 55(15), 2224–2227.

Alexandrova, O., Lacombe, C., and Mangeney, A. (2008), Spectra and anisotropy of magnetic fluctuations in the Earth's magnetosheath: Cluster observations, *Ann. Geophys.*, 26 (11), 3585–3596.

Alexandrova, O., Saur, J., Lacombe, C., Mangeney, A., Mitchell, J., Schwartz, S. J., and Robert, P. (2009), Universality of Solar-Wind Turbulent Spectrum from MHD to Electron Scales, *Phys. Rev. Lett.*, 103(16), 165003.

Alexandrova, O., Lacombe, C., Mangeney, A., Grappin, R., and Maksimovic, M. (2012), Solar wind turbulent spectrum at plasma kinetic scales, *Astrophys. J.*, 760, 121.

Angelopoulos, V., Baumjohann, W., Kennel, C. F., Coronti, F. V., Kivelson, M. G., Pellat, R., et al. (1992), Bursty bulk flows in the inner central plasma sheet, *J. Geophys. Res.*, 97(A4), 4027–4039.

Antonova, E. E., and Ovchinnikov, I. L. (1999), Magnetostatically equilibrated plasma sheet with developed medium-scale turbulence: Structure and implications for substorm dynamics, *J. Geophys. Res.*, 104(A8), 17289–17298.

Balogh, A., Carr, C. M., Acuna, M. H., Dunlop, M. W., Beek, T. J. et al. (2001), The Cluster magnetic field investigation: Overview of inflight performance and initial results, *Ann. Geophys.*, 19, 1207–1217.

Baumjohann, W., Paschmann, G., and Cattell, C. A. (1989), Average plasma properties in the central plasma sheet, *J. Geophys. Res.*, 94, 6597–6606, doi:10.1029/JA094iA06p06597.

Biskamp, D. (1993), *Nonlinear magnetohydrodynamics, Cambridge Monographs on Plasma Physics*, Cambridge University Press, Cambridge, NY.

Borovsky, J. E., Elphic, R. C., Funsten, H. O., and Thomsen, M. F. (1997), The Earth's plasma sheet as a laboratory for turbulence in high-β MHD, *J. Plasma Phys.*, 57(1), 1–34.

Borovsky J. E., and Funsten, H. O. (2003), MHD turbulence in the Earth's plasma sheet: Dynamics, dissipation, and driving, *J. Geophys. Res.*, 108(SMP 9), 1–37, doi:10.1029/2002JA009625.

Borovsky, J. E. and Gary, S. P. (2011), Electron-ion Coulomb scattering and the electron Landau damping of Alfvén waves in the solar wind. *J. Geophys. Res.*, 116, A07101.

Bourouaine, S., Alexandrova, O., Marsch, E. and Maksimovic, M. (2012), On spectral breaks in the power spectra of magnetic fluctuations in fast solar wind between 0.3 and 0.9 AU, *Astrophys. J.*, 749(2), 102.

Breuillard, H., Yordanova, E., Vaivads, A., and Alexandrova, O. (2016) The effects of kinetic instabilities on small-scale turbulence in Earth's magnetosheath, *Astrophys. J.*, 829, 54, doi:10.3847/0004-637X/829/1/54.

Bruno, R., and Carbone, V. (2013), The solar wind as a turbulence laboratory, *Living Rev. Solar Phys.*, 10, 2.

Bruno, R., and Trenchi, L. (2014), Radial dependence of the frequency break between fluid and kinetic scales in the solar wind fluctuations, *Astrophys. J. Lett.*, 787: L24.

Bruno, R., Carbone, V., Veltri, P., Pietropaolo, E., and Bavassano, B. (2001), Identifying intermittency events in the solar wind, *Planet. Space Sci.*, 49(12), 1201–1210.

Bruno, R., Trenchi, L., and Telloni, D. (2014), Spectral slope variation at proton scales from fast to slow solar wind, *Astrophys. J. Lett.*, 793:L15.

Burgess, D., Hellinger, P., Gingell, I., and Travnicek, P. M. (2016), Microstructure in two- and three-dimensional hybrid simulations of perpendicular collisionless shocks, *J. Plasma Phys.*, 82(4), 905820401.

Burlaga, L.F. (1991), Intermittent turbulence in the solar wind, *J. Geophys. Res.*, 96(15), 5847–5851.

Canuto, D., and Taira, K.(2015), Two-dimensional compressible viscous flow around a circular cylinder, *J. Fluid Mech.*, 785, 349–371.

Carbone, F., Sorriso-Valvo, L., Alberti, T., Lepreti, F., Chgen, C.H.K., Nemecek, Z. and Safrankova J. (2018), Arbitrary-order Hilbert spectral analysis and intermittency in solar wind density fluctuations, *Astrophys. J.*, 859, 27, doi:10.3847/1538-4357/aabcc2.

Chang, T. (2001), An example of resonances, coherent structures and topological phase transitions – the origin of the low frequency broadband spectrum in the auroral zone, *Nonlinear Process. Geophys.*, 8, 175–179, doi:10.5194/npg-8-175-2001.

Chang, T. (2015), *An introduction to space plasma complexity*, Cambridge University Press, NY.

Chang, T. and Wu, C. C. (2008), Rank-ordered multifractal spectrum for intermittent fluctuations, *Phys. Rev.*, E77(R), doi:10.1103/045401.

Chang, T., Tam, S. W. Y., and Wu, C. C. (2004), Complexity induced anisotropic bimodal intermittent turbulence in space plasmas, *Phys. Plasmas*, 11, 1287

Chang, T., Wu, C. C., and Podesta, J. (2008), Multifractal characteristics of dynamical complexity in space plasmas. In G. Li, R. P. Lin, J. Luhmann, et al. (Eds.), *Particle acceleration and transport in the heliosphere and beyond* (pp. 75–80), AIP Conference Proceedings, Vol. 1039.

Chang, T., Wu, C. C., Podesta, J., Echim, M., Lamy, H., and Tam, S. W. Y. (2010), ROMA (rank-ordered multifractal analyses) of intermittency in space plasmas – a brief tutorial review, *Nonlinear Process. Geophys.*, 17, 545–551, doi:10.5194/npg-17-545-2010.

Chasapis, A., Retinò, A., Sahraoui, F., Vaivads, A., Khotyaintsev, Yu. V., et al. (2015), Thin current sheets and associated electron heating in turbulent space plasma, *Astrophys. J. Lett.*, 804, L1, doi:10.1088/2041-8205/804/1/L1.

Chasapis, A., Matthaeus, W. H., Parashar, T. N., Le Contel, O., Retinò, A., Breuillard, H., et al. (2017), Electron heating at kinetic scales in magnetosheath turbulence, *Astrophys. J.*, 836, 247, https://doi:10.3847/1538-4357/836/2/247.

Chen, C. H. K., Salem, C. S., Bonnell, J. W., Mozer, F. S., and Bale, S. D. (2012), Density fluctuation spectrum of solar wind turbulence between ion and electron scales, *Phys. Rev. Lett.*, 109, 035001.

Chen, C. H. K., Klein, K. G., and Howes, G. G. (2019), Evidence for electron Landau damping in space plasma turbulence, *Nat. Commun.*, 10, id. 740.

Consolini, G., and Chang, T. S. (2001), Magnetic field topology and criticality in geotail dynamics: relevance to substorm phenomena, *Space Sci. Rev.*, 95(1/2), 309–321.

Consolini, G., Kretzschmar, M., Lui, A. T. Y., Zimbardo, G., and Macek, W. M. (2005), On the magnetic field fluctuations during magnetospheric tail current disruption: A statistical approach, *J. Geophys. Res.*, 110, A07202, doi:10.1029/2004JA010947.

Consolini, G., Materassi, M., Marcucci, M. F., and Pallocchia, G. (2015), Statistics of the velocity gradient tensor in space plasma turbulence flows, *Astrophys. J.*, 812, 84, doi:10.1088/0004-637X/812/1/84.

Cornilleau-Wehrlin, N., Chanteur, G., Perraut, S., Rezeau, L., Robert, P. et al. (2003), First results obtained by the Cluster STAFF experiment, *Ann. Geophys.*, 21, 437–456, http://www.ann-geophys.net/21/437/2003/.

Cousins, E. D. P., and Shepherd, S. G. (2012), Statistical characteristics of small-scale spatial and temporal electric field variability in the high-latitude ionosphere, *J. Geophys. Res.*, 117(A3), id. A03317.

Czaykowska, A., Bauer, T. M., Treumann, R. A., and Baumjohann, W. (2001), Magnetic field fluctuations across the Earth's bow shock, *Ann. Geophys.*, 19, 275–287, http://www.ann-geophys.net/19/275/2001/.

De Camillis, S., Cerri, S. S., Califano, F., and Pegoraro, F. (2016), Pressure anisotropy generation in a magnetized plasma configuration with a shear flow velocity, *Plasma Phys. Controlled Fusion*, 58(4), art. id. 045007.

Dubinin, E., Skalsky, A., Song, P., Savin, S., Kozyra, J., Moore, T. E., et al. (2002), Polar-Interball coordinated observations of plasma and magnetic field characteristics in the regions of the northern and southern distant cusps, *J. Geophys. Res.: Space Phys.*, 107(A5), id. 1053, doi:10.1029/2001JA900068.

Dwivedi, N. K., Kumar, S., Kovacs, P., Yordanova, E., Echim, M., Sharma, R. P., et al, (2019), Implication of kinetic Alfvén waves to magnetic field turbulence spectra: Earth's magnetosheath, *Astrophysics and Space Science*, 364 (6), id. 101, 11 pp., doi: 10.1007/s10509-019-3592-2.

Echim, M. M., and Lemaire, J. F. (2000), Laboratory and numerical simulations of the impulsive penetration mechanism, *Space Sci. Rev.*, 92(3/4), 565–601.

Echim, M. M., Lamy, H., and Chang, T. (2007), Multi-point observations of intermittency in the cusp regions, *Nonlinear Process. Geophys.*, 14, 525–534, doi:10.5194/npg-14-525-2007.

El-Alaoui, M., Richard, R. L., Ashour-Abdalla, M., Goldstein, M. L., and Walker, R. J. (2013), Dipolarization and turbulence in the plasma sheet during a substorm: THEMIS observations and global MHD simulations, *J. Geophys. Res.: Space Phys.*, 118, 7752–7761, doi:10.1002/2013JA019322.

El-Alaoui, M., Richard, R. L., Nishimura, Y., and Walker, R. J. (2016), Forces driving fast flow channels, dipolarizations, and turbulence in the magnetotail, *J. Geophys. Res.: Space Phys.*, 121, 11063–11076, doi:10.1002/2016JA023139.

Ergun, R. E., Goodrich, K. A., Wilder, F. D., Ahmadi, N., Holmes, J. C., Eriksson, S., et al. (2018), Magnetic reconnection, turbulence, and particle acceleration: observations in the Earth's magnetotail, *Geophys. Res. Lett.*, 45(8), 3338–3347.

Farge, M. (1991), Wavelet analysis of coherent structures in two-dimensional turbulent flows, *Phys. Fluids A*, 3(9), 2029.

Frisch, U. (1995), *Turbulence: The legacy of A. N. Kolmogorov*, Cambridge University Press, Cambridge.

Gary, S. P., Convery, P. D., Denton, R. E., Fuselier, S. A., and Anderson, B. J. (1994), Proton and helium cyclotron anisotropy instability thresholds in the magnetosheath, *J. Geophys. Res.*, 99(A4), 5915–5921.

Gentile, V., Schrijer, F. F. J., Van Oudheusden, B. W., and Scarano, F. (2016), Low-frequency behavior of the turbulent axisymmetric near-wake, *Phys. Fluids*, 28(6), 065102.

Gingell, I., Schwartz, S. J., Burgess, D., Johlander, A., Russell, C. T., Burch, J. L., et al. (2017), *J. Geophys. Res.: Space Phys.*, 122(11), 11003–11017.

Goldreich, P., and Sridhar, S. (1995), Toward a theory of interstellar turbulence. 2: Strong Alfvénic turbulence, *Astrophys. J.*, 438(2), 763–775.

Golovchanskaya, I. V., and Kozelov, B. V. (2010), On the origin of electric turbulence in the polar cap ionosphere, *J. Geophys. Res.*, 115(A9), A09321.

Grison, B., Sahraoui, F., Lavraud, B., Chust, T., Cornilleau-Wehrlin, N., Rème, H., et al. (2005), Wave particle interactions in the high-altitude polar cusp: a Cluster case study, *Ann. Geophys.*, 23(12), 3699–3713.

Hasegawa, H., Fujimoto, M., Phan, T. D., Reme, H., A. Balogh, A., Dunlop, M. W., et al. (2004), Transport of solar wind into Earth's magnetosphere through rolled-up Kelvin-Helmholtz vortices, *Nature*, 430(7001), 755–758.

Heikkila, W. J., and Winningham, J. D. (1971), Penetration of magnetosheath plasma to low altitudes through the dayside magnetospheric cusps, *J. Geophys. Res.*, 76(4), 883–891, doi:10.1029/JA076i004p00883.

Hietala, H., and Plaschke, F. (2013), On the generation of magnetosheath high-speed jets by bow shock ripple by bow shock ripples, *J. Geophys. Res.*, 118, 7237–7245.

Hnat, B., Chapman, S, Rowlands, G., and Watkins, N. W. (2002), Finite size scaling in the solar wind magnetic fieldenergy densityas seen by WIND, *Geophys, Res*, *Lett.*, 29, 1446, doi:10.1029/2001GL014587.

Horbury, T. S., Forman, M., and Oughton, S. (2008), Anisotropic scaling of magnetohydrodynamic turbulence, *Phys. Rev. Lett.*, 101, 175005, doi:10.1103/PhysRevLett.101.175005.

Hornig, G., and Schindler, K. (1996), Magnetic topology and the problem of its invariant definition, *Phys. Plasmas*, 3(3), 781–791.

Howes, G. G., Dorland, W., Cowley, S. C., Hammett, G. W., Quataert, E., Schekochihin, A. A., and Tatsuno, T. (2008), Kinetic simulations of magnetized turbulence in astrophysical plasmas, *Phys. Rev. Lett.*, 100(6), 065004.

Howes, G.G., Klein, K. G., and TenBarge, J. M. (2014), Validity of the Taylor hypothesis for linear kinetic waves in the weakly collisional solar wind, *Astrophys. J.*, 789, 2.

Huang, S. Y., Hadid, L. Z., Sahraoui, F., Yuan, Z. G., and Deng, X. H. (2017), On the existence of the Kolmogorov inertial range in the terrestrial magnetosheath turbulence, *Astrophys. J. Lett.*, 836(1), L10.

Hussain, A. K. M. F., and Reynolds, W. C. (1975), Measurements in fully developed turbulent channel flow, *Trans. ASME, Ser. I: J. Fluids Eng.*, 97, 568–578.

Iroshnikov, P. S. (1963), Turbulence of conducting fluids in a strong magnetic field, *Sov. Astron.*, 7, 566–571.

Jasperse, J. R., Basu, B., Lund, E. J., and Bouhram, M. (2006a), Gyrotropic guiding center fluid theory for turbulent inhomogeneous, magnetized plasma, *Phys. Plasmas*, 13, 072903.

Jasperse, J. R., Basu, B., Lund, E. J., and Bouhram, M. (2006b), Gyrotropic guiding center fluid theory for turbulent heating of magnetospheric ions in downward Birkland current regions. II, *Phys. Plasmas*, 13, 112902.

Johlander, A., Schwartz, S. J., Vaivads, A., YKhotyaintsev, Y. V., Gingell, I., Peng, I. B., et al. (2016), Rippled quasiperpendicular shock observed by the Magnetospheric Multiscale Spacecraft, *Phys. Rev. Lett.*, 117, 165101.

Johlander, A. Vaivads, A., Khotyaintsev, Y. V., Gingell, I., Schwartz, S. J., Giles, B. L., et al. (2018), Shock ripples observed by the MMS spacecraft: ion reflection and dispersive properties, *Plasma Phys. Control. Fusion*, 60, 125006, doi:10.1088/1361-6587/aae920.

Johnson, J. R., and Cheng, C. Z. (2001), Stochastic ion heating at the magnetopause due to kinetic Alfvén waves. *Geophys. Res. Lett.*, 28, 4421–4424.

Johnson, J. R., Wing, S., and Delamere, P. A. (2014), Kelvin Helmholtz instability in planetary magnetospheres, *Space Sci. Rev.*, 184(1–4), 1–31.

Kadanoff, L. P., Götze, W., Hamblen, D., Hecht, R., Lewis, E. A., Palciauskas, V. V., et al. (1967), Static phenomena near critical points: Theory and experiment, *Rev. Mod. Phys.*, 39 (2), 395–431.

Kajdic, P., Blanco-Cano, X., Omidi, N., Rojas-Castillo, D., Sibeck, D. G., Billingham, L. (2017), Traveling foreshocks and transient foreshock phenomena. *J. Geophys. Res.: Space Phys.*, 122, 9148–9168, doi:10.1002/2017JA023901.

Karimabadi, H., Roytershteyn, V., Hu, X., Omelchenko, Y. A., Scudder, J., Daughton, W., et al. (2014), The link between shocks, turbulence, and magnetic reconnection in collisionless plasmas, *Phys. Plasmas*, 21, 062308, doi:10.1063/1.4882875.

Khotyaintsev, Y., Vaivads, A., Ogawa, Y., Popielawska, B., André, M., Buchert, S., et al. (2004), Cluster observations of high-frequency waves in the exterior cusp, *Ann. Geophys.*, 22(7), 2403–2411, doi:10.5194/angeo-22-2403-2004.

Kintner, P.M. (1976), Observations of velocity shear driven plasma turbulence, *J. Geophys. Res.*, 81, 5114–5122.

Kiyani, K. H., Chapman, S. C., Khotyaintesev, Y. V., Dunlop, M. W., and Sahraoui, F. (2009), Global scale-invariant dissipation in collisionless plasma turbulence, *Phys. Rev. Lett.*, 103, 075006, doi:10.1103/PhysRevLett.103.075006.

Kolmogorov, A. N. (1941), The local structure of turbulence in incompressible viscous fluid for very large Reynolds number, *Dokl. Akad. Nauk. SSSR*, 30, 299–303 (Reprinted 1991 in *Proc. Roy. Soc. A*, 434, 9–13, doi:10.1098/rspa.1991.0075).

Kovács, P., Carbone, V., and Vörös, Z. (2001), Wavelet-based filtering of intermittent events from geomagnetic time-series, *Planet. Space Sci.*, 49, 1219–1231, doi:10.1016/S0032-0633(01)00063-0.

Kraichnan, R. (1965a), Lagrangian-history closure approximation for turbulence, *Phys. Fluids*, 8, 575–598, doi:10.1063/1.1761271.

Kraichnan, R. (1965b), Inertial-range spectrum of hydromagnetic turbulence, *Phys. Fluids*, 8, 1385–1387, doi:10.1063/1.1761412.

Kretzschmar, M., and Consolini, G. (2006), Complexity in the Erath's magnetotail plasma sheet, *Adv. Space Res.*, 37, 552–558, doi:10.10106/j.asr.2005.03.063.

Lacombe, C., Alexandrova, O., and Matteini, L. (2017), Anisotropies of the magnetic field fluctuations at kinetic scales in the solar wind: Cluster observations, *Astrophys. J.*, 848, 1.

Lakhina, G. S. (1990), Generation of ULF waves in the polar cusp region by velocity shear-driven kinetic Alfvén modes, *Astrophys. Space Sci.*, 165(1), 153–161, doi:10.1007/BF00653667.

Lapenta, G., Pucci, F., Olshevsky, V., Servidio, S., Sorriso-Valvo, L., Newman, D. L., and Goldman, M. V. (2018), Nonlinear waves and instabilities leading to secondary reconnection in reconnection outflows, *J. Plasma Phys.*, 84(1), art. id. 715840103.

Le, G., Blanco-Cano, X., Russell, C. T., Zhou, X.-W., Mozer, F., Trattner, K. J., et al. (2001), Electromagnetic ion cyclotron waves in the high-altitude cusp-Polar observations, *J. Geophys. Res.*, 106(A9), 19067–19079.

Leamon, R. J., Smith, C. W., Ness, N. F., Matthaeus, W. H., and Wong, H. K. (1998), Observational constraints on the dynamics of the interplanetary magnetic field dissipation range, *J. Geophys. Res.*, 103(A3), 4775–4787.

Leamon, R. J., Smith, C. W., Ness, N. F., and Wong, H. K. (1999), Dissipation range dynamics: Kinetic Alfvén waves and the importance of βe, *J. Geophys. Res.*, 104(A10), 22331–22344.

Leamon, R. J., Matthaeus, W. H., Smith, C. W., Zank, G. P., Mullan, D. J., and Oughton, S. (2010), MHD-driven kinetic dissipation in the solar wind and corona, *Astrophys. J.*, 537 (2), 1054–1062.

Liu, J., and Horton, W. (1986), The intrinsic electromagnetic solitary vortices in magnetized plasma. *J. Plasma Phys.*, 36, 1–24.

Loureiro, N. F., and Boldyrev, S. (2017), Role of magnetic reconnection in magnetohydrodynamic turbulence, *Phys. Rev. Lett.*, 118(24), id.245101.

Lundin, R., and Dubinin, E.M. (1985), Solar wind energy transfer regions inside the dayside magnetopause: Accelerated heavy ions as tracers for MHD-processes in the dayside boundary layer, *Planet. Space Sci.*, 33(8), 891–890.

Macek, W. M., and Wawrzaszek A. (2011), Multifractal two-scale Cantor set model for slow solar wind turbulence in the outer heliosphere during solar maximum, *Nonlinear Process. Geophys.*, 18, 287–294.

Macek, W. M., Wawrzaszek, A., and Sibeck, D. G. (2015), THEMIS observation of intermittent turbulence behind the quasi-parallel and quasi-perpendicular shocks, *J. Geophys. Res.: Space Phys.*, 120, 7466–7476, doi:10.1002/2015JA021656.

Macek, W. M., Krasińska, A., Silveira, M. V. D., Sibeck, D. G., Wawrzaszek, A., Burch, J. L., and Russell, C. T. (2018a), Magnetospheric Multiscale observation of turbulence in the magnetosheath on kinetic scales, *Astrophys. J. Lett.*, 864, L29.

Macek, W. M., Wawrzaszek, A., and Kucharuk, B. (2018b), Intermittent turbulence in the heliosheath and the magnetosheath plasmas based on Voyager and THEMIS data, *Nonlinear Process. Geophys.*, 25(1), 39–54.

Mallat, S., and Zhong, S. (1992), Characterization of signals from multiscale edges, *IEEE Trans. Pattern Anal. Mach. Intell.*, 14, 710–732.

Mangeney, A., Lacombe, C., Maksimovic, M., Samsonov, A. A., Cornilleau-Wehrlin, N., Harvey, C. C., et al. (2006), Cluster observations in the magnetosheath – Part 1: Anisotropies of the wave vector distribution of the turbulence at electron scales, *Ann. Geophys.*, 24(12), 3507–3521.

Marsch, E., and Tu, C. Y. (1994), Non-Gaussian probability distributions of solar wind fluctuations, *Ann. Geophys.*, 12, 1127–1138, doi:10.1007/s00585-994-1127-8.

Matthaeus, W. H., and Lamkin, S. L. (1986), Turbulent magnetic reconnection, *Phys. Fluids*, 29, 2513–2534.

Matthaeus, W.H., and Goldstein, M.L. (1986), Low-frequency 1/f noise in the interplanetary magnetic field, *Phys. Rev. Lett.*, 57(4), 495–498, doi:10.1103/PhysRevLett.57.495.

Milovanov, A. V., Zelenyi, L. M., Zimbardo, G., and Veltri, P. (2001), Self-organized branching of magnetotail current systems near the percolation threshold, *J. Geophys. Res.*, 106, 6291–6307, doi:10.1029/1999JA000446.

Motschmann, U., Woodward, T. I., Glassmeier, K. H., Southwood, D. J., and Pinçon, J. L. (1996), Wavelength and direction filtering by magnetic measurements at satellite arrays: Generalized minimum variance analysis, *J. Geophys. Res.*, 101(A3), 4961–4966.

Nakamura, R., Baumjohann, W., Mouikis, C., Kistler, L. M., Runov, A., Volwerk, M., et al. (2004), Spatial scale of high-speed flows in the plasma sheet observed by Cluster, *Geophys. Res. Lett.*, 31(9), doi:10.1029/2004GL019558.

Narita, Y. (2015), Non-elliptic wavevector anisotropy for magnetohydrodynamic turbulence, *Ann. Geophys.*, 33, 1413–1419, doi:10.5194/angeo-33-1413-2015.

Narita, Y. (2016a), Kinetic extension of critical balance to whistler turbulence, *Astrophys. J.*, 831, 83, doi:10.3847/0004-637X/831/1/83.

Narita, Y. (2016b), Cluster observation of magnetohydrodynamic turbulence in the plasma sheet boundary layer, *Earth, Planets Space*, 68, 69, doi:10.1186/s40623-016-0442-0.

Narita, Y. (2017), Review article: Wave analysis methods for space plasma experiment, *Nonlinear Process. Geophys.*, 24, 203–214, doi:10.5194/npg-24-203-2017.

Narita, Y., Nakamura, R., Baumjohann, W., Glassmeier, K.-H., Motschmann, U., and Comişel, H. (2016), Ion Bernstein waves in the magnetic reconnection region, *Ann. Geophys.*, 34, 85–89, doi:10.5194/angeo-34-85-2016.

Neagu, E., Borovsky, J. E., Thomsen, M. F., Gary, S. P., Baumjohann, W., and Treumann, R. A. (2002), Statistical survey of magnetic field and ion velocity fluctuations in the near-Earth plasma sheet: Active Magnetospheric Particle Trace Explorers/Ion Release Module (AMPTE/IRM) measurements, *J. Geophys. Res.*, 107, SMP 8 1–10, doi:10.1029/2001JA000318.

Neagu, E., Borovsky, J. E., Gary, S. P., Jorgensen, A. M., Baumjohann, W., and Treumann, R. A. (2005), Statistical survey of magnetic and velocity fluctuations in the near-Earth plasma sheet: International Sun Earth Explorer (ISEE-2) measurements, *J. Geophys. Res.: Space Phys.*, 110(A5), A05203.

Nykyri, K., Grison, B., Cargill, P. J., Lavraud, B., Lucek, E., Dandouras, I., et al. (2006), Origin of the turbulent spectra in the high-altitude cusp: Cluster spacecraft observations, *Ann. Geophys.*, 24, 1057–1075, doi:10.5194/angeo-24-1057-2006.

Nykyri, K., Otto, A., Adamson, E., Tjulin, A. (2011), On the origin of fluctuations in the cusp diamagnetic cavity, *J. Geophys. Res.*, 116(A6), id. A06208.

Osman, K. T., Matthaeus, W. H., Greco, A., and Servidio, S. (2011), Evidence for inhomogeneous heating in the solar wind. *Astrophys. J.*, 727, L11, doi:10.1088/2041-8205/727/1/L11.

Ovchinnikov, I. L., and Antonova, E. E. (2017), Turbulent transport of the Earth magnetosphere: Review of the results of observations and modeling, *Geomagn. Aeron.*, 57(6), 655–663.

Perri S., Goldstein, W. L., Dorelli, J. C., and Sahraoui, F. (2012), Detection of small-scale structures in the dissipation regime of solar-wind turbulence, *Phys. Rev. Lett.* 109, 191101.

Perri S., Servidio S., Vaivads A., and Valentini F. (2017), Numerical study on the validity of the Taylor hypothesis in space plasmas, *Astrophys. J. (Supplement Series)*, 231, 1.

Petkaki, P., Freeman, M. P., and Walsh, A. P. (2006), Cluster observations of broadband electromagneticaround a reconnection region in the Earth'swaves in and magnetotail current sheet, *Geophys. Res. Lett.*, 33, L16105, doi:10.1029/2006GL027066.

Petviashvili, V. I., and Pokhotelov, O. A. (1992), *Solitary waves in plasma and in the atmosphere*, Gordon & Breach Science Pub.

Phan, T. D., Paschmann, G., Twitty, C., Mozer, F. S., Gosling, J. T., Eastwood, J. P., et al. (2007), Evidence for magnetic reconnection initiated in the magnetosheath, *Geophys. Res. Lett.*, 34, L14104. doi:10.1029/2007GL030343.

Pickett, J. S., Franz, J. R., Scudder, J. D., Menietti, J. D., Gurnett, D. A., Hospodarsky, G. B., et al. (2001), Plasma waves observed in the cusp turbulent boundary layer: An analysis of high time resolution wave and particle measurements from the Polar spacecraft, *J. Geophys. Res.*, 106(A9), 19081–19099, doi:10.1029/2000JA003012.

Pincon, J. L., and Lefeuvre, F. (1991), Local characterization of homogeneous turbulence in a space plasma from simultaneous measurements of field components at several points in space, *J. Geophys. Res.*, 96, 1789–1802.

Quattrociocchi, V., Consolini, G., Marcucci, M.F., Materassi, M. (2019), On geometrical invariants of the magnetic field gradient tensor in turbulent space plasmas: Scale variability in the inertial range. *The Astrophysical Journal*, 878(124), https://doi.org/10.3847/1538–4357/ab1e47.

Retinò, A., Sundkvist, D., Vaivads, A., Mozer, F., André, M., and Owen, C. J. (2007), In situ evidence of magnetic reconnection in turbulent plasma, *Nature Phys.*, 3, 236–238, doi:10.1038/nphys574.

Richardson, L.F. (1922), *Weather prediction by numerical process*, Cambridge University Press, OCLC 3494280.

Rojas-Castillo, D., Blanco-Cano, X. Kajdič, P., and Omidi, N. (2013), Foreshock compressional boundaries observed by Cluster. *J. Geophys. Res.*, 118, 698–715, https://doi.org/10.1029/2011JA017385.

Saddoughi, S. G., and Veeravalli, S. V. (1994), Local isotropy in turbulent boundary layers at high Reynolds number, *J. Fluid Mech.*, 268, 333–372, doi:10.1017/S0022112094001370.

Sahraoui, F., Pinçon, J. L., Belmont, G., Rezeau, L., Cornilleau-Wehrlin, N., Robert, P., et al. (2003), ULF wave identification in the magnetosheath: The k-filtering technique applied to Cluster II data, *J. Geophys. Res.: Space Phys.*, 108, SMP 1, 1–19, id. 1335, doi:10.1029/2002JA009587.

Sahraoui, F., Belmont, G., Rezeau, L., Cornilleau-Wehrlin, N., Pinçon, J. L., and Balogh, A. (2006), Anisotropic turbulent spectra in the terrestrial magnetosheath as seen by the Cluster spacecraft, *Phys. Rev. Lett.*, 96, 075002, doi:10.1103/PhysRevLett.96.075002.

Sahraoui, F., Goldstein, M. L., Robert, P., and Khotyaintsev, Y. V. (2009), Evidence of a Cascade and dissipation of solar-wind turbulence at the electron gyroscale, *Phys. Rev. Lett.*, 102, 231102.

Sahraoui, F., Goldstein, M. L., Belmont, G., Canu, P., and Rezeau, L. (2010), Three dimensional anisotropic k spectra of turbulence at subproton scales in the solar wind, *Phys. Rev. Lett.*, 105, 131101.

Savin,S. P., Borodkova, N. L., Budnik, A., Fedorov, A. O., Klimov, S. I., Nozdrachev, M. N., et al. (1998), Interball tail probe measurements in outer cusp and boundary layers. In J. L. Horwitz, D. L. Gallagher, and W. K. Peterson (Eds.), *Geospace mass and energy flow: Results from the international solar-terrestrial physics program*, Geophysical Monograph Series, vol. 104, AGU, Washington, DC.

Savin, S., Büchner, J., Consolini, G., Nikutowski, B., Zelenyi, L., Amata, E., et al. (2002), On the properties of turbulent boundary layer over polar cusps, *Nonlinear Process. Geophys.*, 9(5/6), 443–451.

Schekochihin, A. A., Cowley, S. C., Dorland, W., Hammett, G. W., Howes, G. G., Plunk, G. G., et al. (2008), Gyrokinetic turbulence: a nonlinear route to dissipation through phase space, *Plasma Phys. Control. Fusion*, 50(12), id. 124024.

Schekochihin, A. A., Cowley, S. C., Dorland, W., Hammett, G. W., Howes, G. G., Quataert, E., and Tatsuno, T. (2009), Astrophysical gyrokinetics: Kinetic and fluid turbulent cascades in magnetized weakly collisional plasmas, *Astrophys. J., Suppl. Ser.*, 182(1), 310–377.

Schwartz, S. J., Burgess, D., Wilkinson, W. P., Kessel, R. L., Dunlop, M., and Lühr, H. (1992), Observations of short large-amplitude magnetic structures at a quasi-parallel shock, *J. Geophys. Res.*, 97(A4), 4209–4227.

Schwartz, S. J., Burgess, D., and Moses, J. J. (1996), Low-frequency waves in the Earth's magnetosheath: present status, *Ann. Geophys.*, 14, 1134–1150, doi:10.1007/s00585-996-1134-z.

Sergeev, V., Kubyshkina, M., Alexeev, I., Fazakerley, A., Owen, C., Baumjohann, W., et al. (2008), Study on near-Earth reconnection events with Cluster and Double Star, *J. Geophys. Res.: Space Phys.*, 113, A07S36, doi:10.1029/2007JA012902.

Servidio, S., Valentini, F., Califano, F., and Veltri, P. (2012), Local kinetic effects in two-dimensional plasma turbulence, *Phys. Rev. Lett.*, 108(4), id. 045001.

Shukla, P. K., Yu, M. Y., and Stenflo, L. (1986), Electromagnetic drift vortices. *Phys. Rev. A*, 34, 3478–3480.

Sorriso-Valvo, L., Carbone, V., Veltri, P., Consolini, G., and Bruno, R. (1999), Intermittency in the solar wind turbulence through probability distribution functions of fluctuations. *Geophys. Res. Lett.*, 26, 1801–1804.

Sorriso-Valvo, L., Yordanova, E., and Carbone, V. (2010), On the scaling properties of anisotropy of interplanetary magnetic turbulent fluctuations, *Europhys. Lett.*, 90, 59001.

Stawarz, J. E., Ergun, R. E., and Goodrich, K.A. (2015), Generation of high-frequency electric field activity by turbulence in the Earth's magnetotail, *J. Geophys. Res.: Space Phys.*, 120, 1845–1866, doi:10.1002/2014JA020166.

Stawicki, O., Gary, S. P., and H. Li (2001), Solar wind magnetic fluctuation spectra: Dispersion versus damping, *J. Geophys. Res.*, 106(A5), 8273–8282.

Stepanova, M., Pinto, V., Valdivia, J. A., and Antonova, E. E. (2011) Spatial distribution of the eddy diffusion coefficients in the plasma sheet during quiet time and substorms from THEMIS satellite data, *J. Geophys. Res.*, 116, A00I24, doi:10.1029/2010JA015887.

Sundkvist, D., Krasnoselskikh, V., Shukla, P. D., Vaivads, A., André, M., Buchert, S., and Rème, H. (2005), In situ multi-satellite detection of coherent vortices as a manifestation of Alfvénic turbulence, *Nature*, 436, 825–828, doi:10.1038/nature03931.

Sundkvist, D., Retino, A., Vaivads, A., and Bale, S. D. (2007), Dissipation in turbulent plasma due to reconnection in thin current sheets. *Phys. Rev. Lett.*, 99, 025004.

Tam, S.W.Y., and Chang, T. (2011), Double rank-ordering technique of ROMA (Rank-Ordered Multifractal Analysis) for multifractal fluctuations featuring multiple regimes of scales, *Nonlinear Proces. Geophys.*, 18, 405–414.

Tam, S. W. Y., Chang, T., Kintner, P. M., and Klatt, E. (2005), Intermittency analyses on the SIERRA measurements of the electric field fluctuations in the auroral zone, *Geophys. Res. Lett.*, 32, L05109, doi:10.1029/2004GL 021445.

Tam, S. W. Y., Chang, T., Kintner, P. M., and Klatt, E. M. (2010) Rank-ordered multifractal analysis for intermittent fluctuations with global crossover behavior, *Phys. Rev. E.*, 81, 036414.

Taneda, S. (1956), Experimental investigation of the wakes behind cylinders and plates at low Reynolds numbers, *J. Phys. Soc. Jpn.*, 11(3), 302–307.

Taylor, G. I. (1938), The spectrum of turbulence, *Proc. R. Soc. Lond. A*, 164, 476–490, doi:10.1098/rspa.1938.0032.

Valentini, F., Servidio, S., Perrone, D., Califano, F., Matthaeus, W. H., and Veltri, P. (2014), Hybrid Vlasov-Maxwell simulations of two-dimensional turbulence in plasmas, *Phys. Plasmas*, 21(8), 082307.

Voitenko, Y., and Goossens, M. (2004), Cross-field heating of coronal ions by low frequency kinetic Alfvén waves. *Astrophys. J.*, 605, L149–L152.

Vörös, Z., Baumjohann, W., Nakamura, R., Volwerk, M., Runov, A., Zhang, T. L., et al. (2004), Magnetic turbulence in the plasma sheet, *J. Geophys. Res.: Space Phys.*, 109, A11215, doi:10.1029/2004JA010404.

Vörös, Z., Baumjohann, W., Nakamura, R., Runov, A., Volwerk, M., Takada, T.,et al. (2007a), Spatial structure of plasma flow associated turbulence in the Earth's plasma sheet, *Ann. Geophys.*, 25, 13–17, doi:10.5194/angeo-25-13-2007.

Vörös, Z., Baumjohann, W., Nakamura, R., Runov, A., Volwerk, M., Asano, Y., et al. (2007b), Spectral scaling in the turbulent Earth's plasma sheet revisited, *Nonlinear Process. Geophys.*, 14, 535–541, doi:10.5194/npg-14-535-2007.

Vörös, Z., Nakamura, R., Sergeev, V., Baumjohann, W., Runov, A., Zhang, T. L., et al. (2008), Study of reconnection-associated multiscale fluctuations with Cluster and Double Star, *J. Geophys. Res.: Space Phys.*, 113, A07S29, doi:10.1029/2007JA012688.

Vörös, Z., Yordanova, E., Echim, M. M., Consolini, G., and Narita, Y. (2016), Turbulence-generated proton-scale structures in the terrestrial magnetosheath, *Astrophys. J. Lett.*, 819, L15, doi:10.3847/2041-8205/819/1/L15.

Vörös, Z., Yordanova, E., Varsani, A., Genestreti, K. J., Khotyaintsev, Yu. V., et al. (2017), MMS observation of magnetic reconnection in the turbulent magnetosheath, *J. Geophys. Res.: Space Phys.*, 122, doi:10.1002/2017JA024535.

Walsh, B. M., Fritz, T. A., and Chen, J. (2012), Simultaneous observations of the exterior cusp region, *J. Atmos. Sol. Terr. Phys.*, 87, 47–55.

Walsh, B. M., Thomas, E. G., Hwang, K.-J., Baker, J. B. H., Ruohoniemi, J. M., and Bonnell, J. W. (2015), Dense plasma and Kelvin-Helmholtz waves at Earth's dayside magnetopause, *J. Geophys. Res.: Space Phys.*, 120(7), 5560–5573.

Wan M., Matthaeus, W. H., Karimabadi, H., Roytershteyn, V., Shay, M., Wu, P., et al. (2012), Intermittent dissipation at kinetic scales in collisionless plasma turbulence, *Phys. Rev. Lett.*, 109, 195001.

Wang, T., Cao, J.-B., Fu, H., Liu, W., and Dunlop, M. (2014), Turbulence in the Earth's cusp region: The k-filtering analysis, *J. Geophys. Res.: Space Phys.*, 119, 9527–9542, doi:10.1002/2014JA019997.

Wang, T., Cao, J., Fu, H., Meng, X., and Dunlop, M. (2016), Compressible turbulence with slow-mode waves observed in the bursty bulk flow of plasma sheet, *Geophys. Res. Lett.*, 43, 1854–1861, doi:10.1002/2016GL068147.

Wawrzaszek, A., Echim, M., Macek, W. M., and Bruno, R. (2015), Evolution of intermittency in the slow and fast solar wind beyond the ecliptic plane, *Astrophys. J. Lett.*, 814: L19. doi:10.1088/2041-8205/814/2/L19.

Wawrzaszek, A., Echim, M., and Bruno, R. (2019), Multifractal analysis of heliospheric magnetic field fluctuations observed by Ulysses, *Astrophys. J.*, 876(2), 153, doi:10.3847/1538–4357/ab1750.

Weygand, J. M., Kivelson, M. G., Khurana, K. K.,Schwarzl, H. K., Thompson, S. M., McPherron, R. L., et al. (2005), Plasma sheet turbulence observed by Cluster II, *J. Geophys. Res.: Space Phys.*, 110, A01205, doi:10.1029/2004JA010581.

Weygand, J. M., Matthaeus, W. H., El-Alaoui, M., Dasso, S., and Kivelson, M. G. (2010), Anisotropy of the Taylor scale and the correlation scale in plasma sheet magnetic field

fluctuations as a function of auroral electrojet activity, *J. Geophys. Res.: Space Phys.*, 115(A12), A12250.

Wicks, R. T., Horbury, T. S., Chen, C. H. K., and Schekochihin, A. A. (2010), Power and spectral index anisotropy of the entire inertial range of turbulence in the fast solar wind, *Mon. Not. R. Astron. Soc.*, 407(1), L31–L35.

Woch, J., and Lundin, R. (1992), Magnetosheath plasma precipitation in the polar cusp and its control by the interplanetary magnetic field, *J. Geophys. Res.*, 97, 1421–1430.

Wu, C.C., and Chang, T. (2001), Further study of the dynamics of two-dimensional MHD coherent structures – a large scale simulation, *J. Atmos. Sol. Terr. Phys.*, 63, 1447–1453.

Yordanova, E., Grzesiak, M., Wernik, A. W., Popielawska, B., and Stasiewicz, K. (2004), Multifractal structure of turbulence in the magnetospheric cusp, *Ann. Geophys.*, 22, 2431–2440.

Yordanova, E., Bergman, J., Consolini, G., Kretzschmar, M., Materassi, M., Popielawska, B., et al. (2005), Anisotropic scaling features and complexity in magnetospheric-cusp: a case study, Nonlinear Process. *Geophys.*, 12(6), 817–825.

Yordanova, E., Vaivads, A., André, M., Buchert, S. C. and Vörös Z. (2008),Magnetosheath plasma turbulence andits spatiotemporal evolution as observed by the Cluster spacecraft, *Phys. Rev. Lett.*, 100, 205003, doi:10.1103/PhysRevLett.100. 205003

Yordanova, E., Vörös, Z., Varsani, A., Graham, D. B., Norgren, C., Khotyaintsev, Y. V., et al. (2016), Electron scale structures and magnetic reconnection signatures in the turbulent magnetosheath, *Geophys. Res. Lett.*, 43, 5969–5978, doi:10.1002/2016GL069191.

Yoshizawa, A. (1984), Statistical analysis of the deviation of the Reynolds stress from its eddy-viscosity representation, *Phys. Fluids*, 27, 1377–1387, doi:10.1063/1.864780.

Yoshizawa, A. (1998), Two-scale direct interaction approximation. In A. Yoshizawa, *Hydrodynamic and magnetohydrodynamic turblent flows* (pp. 173–253), Fluid Mechanics and Its Applications, vol. 48, Springer, Dortrecht, doi:10.1007/978-94-017-1810-3_6.

Zhang, H., et al. (2013), Spontaneous hot flow anomalies at quasi-parallel shocks: 1. Observations, *J. Geophys. Res.: Space Phys.*, 118, 3357–3363, doi:10.1002/jgra.50376.

Zimbardo, G., Greco, A., Sorriso-Valvo, L., Perri, S., Vörös, Z., Aburjania, G., et al. (2010), Magnetic turbulence in the geospace environment, *Space Sci. Rev.*, 156, 89–134, doi:10.1007/s11214-010-9692-5.